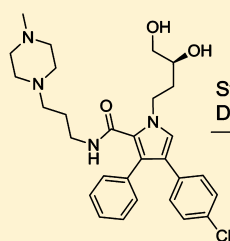


Design of Bcl-2 and Bcl-xL Inhibitors with Subnanomolar Binding Affinities Based upon a New Scaffold[†]

Haibin Zhou,^{‡,§} Jianfang Chen,^{‡,§} Jennifer L. Meagher,^{||,§} Chao-Yie Yang,^{‡,§} Angelo Aguilar,^{‡,§} Liu Liu,^{‡,§} Longchuan Bai,^{‡,§} Xin Cong,[‡] Qian Cai,[‡] Xueliang Fang,[‡] Jeanne A. Stuckey,^{||} and Shaomeng Wang^{*,‡}

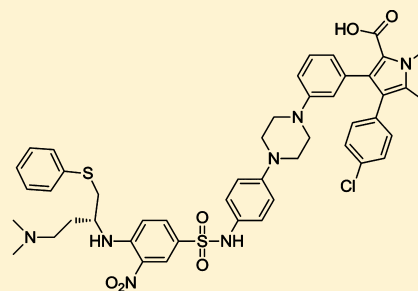
[‡]Comprehensive Cancer Center and Departments of Internal Medicine, Pharmacology, and Medicinal Chemistry and ^{||}Life Sciences Institute, University of Michigan, 1500 East Medical Center Drive, Ann Arbor, Michigan 48109-0934, United States

S Supporting Information



4 (Initial Lead, $K_i = 100 \mu\text{M}$ to Bcl-2/Bcl-xL)

Structure-based Scaffold
 Design and Optimization



21 ($K_i < 1 \text{ nM}$ to Bcl-2/Bcl-xL)

ABSTRACT: Employing a structure-based strategy, we have designed a new class of potent small-molecule inhibitors of the anti-apoptotic proteins Bcl-2 and Bcl-xL. An initial lead compound with a new scaffold was designed based upon the crystal structure of Bcl-xL and U.S. Food and Drug Administration (FDA) approved drugs and was found to have an affinity of $100 \mu\text{M}$ for both Bcl-2 and Bcl-xL. Linking this weak lead to another weak-affinity fragment derived from Abbott's ABT-737 led to an improvement of the binding affinity by a factor of $>10\,000$. Further optimization ultimately yielded compounds with subnanomolar binding affinities for both Bcl-2 and Bcl-xL and potent cellular activity. The best compound (**21**) binds to Bcl-xL and Bcl-2 with $K_i < 1 \text{ nM}$, inhibits cell growth in the H146 and H1417 small-cell lung cancer cell lines with IC_{50} values of $60\text{--}90 \text{ nM}$, and induces robust cell death in the H146 cancer cell line at $30\text{--}100 \text{ nM}$.

INTRODUCTION

Resistance to apoptosis is a hallmark of human cancer,¹ and targeting key apoptosis regulators with the goal of promoting apoptosis is an exciting therapeutic strategy for cancer treatment.^{2,3}

The Bcl-2 protein family is a class of key apoptosis regulators and consists of both anti-apoptotic proteins, including Bcl-2, Bcl-xL, and Mcl-1, and pro-apoptotic proteins, such as BID, BIM, BAD, BAK, BAX, and NOXA.⁴ The anti-apoptotic Bcl-2 and Bcl-xL proteins are overexpressed in many different types of human tumor samples and cancer cell lines, and this overexpression confers resistance of cancer cells to current cancer treatments.^{5,6} The anti-apoptotic proteins inhibit apoptosis via heterodimerization with pro-apoptotic Bcl-2 family proteins.^{5,6} Despite their structural similarities, these anti-death Bcl-2 proteins display a certain binding specificity on pro-death Bcl-2 proteins.^{5,6} For example, while Bcl-2 and Bcl-xL bind to BIM and BAD proteins with high affinities, they have very weak affinities for NOXA. In contrast, Mcl-1 binds to BIM and NOXA with high affinities but has a very weak affinity for BAD. These data suggest that the pro-apoptotic proteins have nonredundant roles in the regulation of apoptosis.

It has been proposed that potent nonpeptide small molecules designed to block the protein–protein interactions between

anti- and pro-apoptotic Bcl-2 members can antagonize the anti-death function of anti-apoptotic Bcl-2 proteins, and this in turn can overcome the apoptosis resistance of cancer cells mediated by the overexpression of these anti-apoptotic Bcl-2 proteins.^{5,6} Design of potent nonpeptide cell-permeable small-molecule inhibitors with the ability to block the protein–protein interactions involving the Bcl-2 family of proteins has been intensely pursued in the past decade as a novel cancer therapeutic strategy, and a number of laboratories have reported the design and characterization of nonpeptide small-molecule inhibitors.^{7–12}

Among all the reported Bcl-2/Bcl-xL inhibitors, compound **1** (ABT-737, Figure 1) is arguably the most potent compound.¹³ Compound **1** binds to Bcl-2, Bcl-xL, and Bcl-w with very high affinities ($K_i < 1 \text{ nM}$) and also shows a very high specificity over Mcl-1 and A1.¹³ Its analogue, **2** (ABT-263, Figure 1), has been advanced into phase I/II clinical trials for the treatment of human cancer.^{14,15} Recently, another class of potent Bcl-2/Bcl-xL inhibitors, exemplified by compound **3** (Figure 1), was designed starting from the chemical structure of compound **1**.¹⁶

Received: February 8, 2012

Published: March 26, 2012

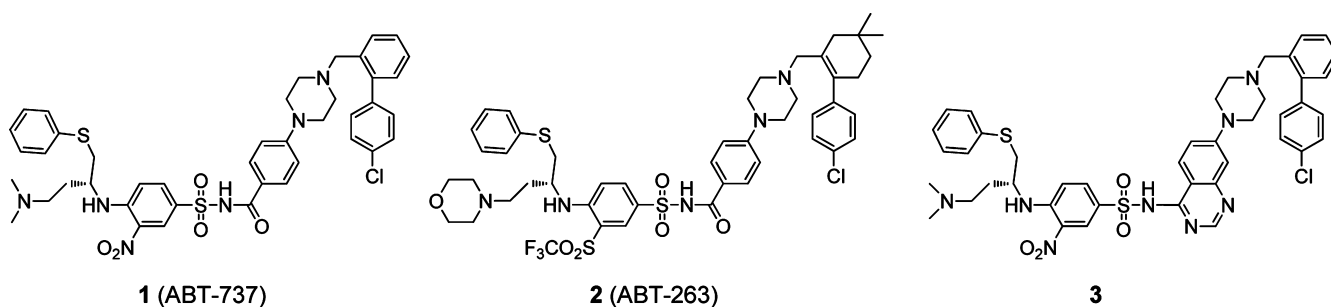


Figure 1. Chemical structures of previously reported potent and specific Bcl-2/Bcl-xL inhibitors.

In this paper, we report our structure-based design of highly potent and specific small-molecule inhibitors of Bcl-2/Bcl-xL, started from a novel chemical scaffold designed based upon FDA-approved drugs and the crystal structures of Bcl-xL complexed with its inhibitors.

RESULTS AND DISCUSSION

Structure-Based Design of a New Chemical Scaffold to Target Bcl-xL. The crystal structure of Bcl-xL complexed with the BAD BH3 peptide¹⁷ reveals that the peptide interacts with two large binding pockets in Bcl-xL, shown in Figure 2.

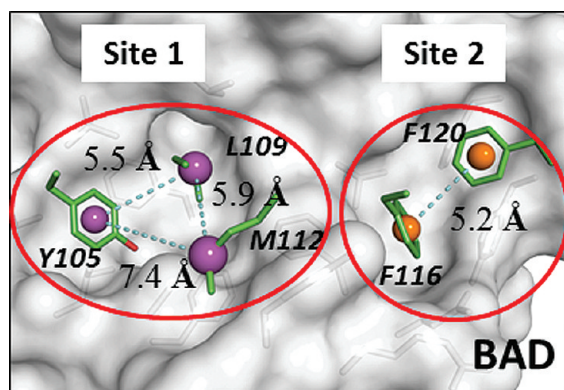


Figure 2. Crystal structure of Bcl-xL with five key residues of BAD BH3 peptide at the binding site. Centroids of hydrophobic pharmacophores are shown as spheres. The pharmacophore model based on three residues at site 1 binding pocket (purple spheres within red circle) was used in pharmacophore search.

Site 1 is a deep, well-defined binding pocket, while site 2 is more exposed to solvents. We decided to focus on site 1 for the design of initial lead compounds with novel chemical scaffolds.

Site 1 of Bcl-xL interacts with Y105, L109, and M112, three hydrophobic residues of the BAD BH3 peptide. The distances between centers of mass of the side chains of any two of these three residues are between 5.5 and 7.4 Å (Figure 2). These three closely clustered hydrophobic residues in the BAD BH3 peptide offer a 3D pharmacophore template, which we used to search for new scaffolds. A pharmacophore model was constructed from these three hydrophobic residues and the structural information, which consists of two aromatic rings and one hydrophobic group. The distance between the centers of the two aromatic rings was defined as 5 ± 1 Å, and the distance between the center of each of the aromatic rings and the center of mass of the hydrophobic group was set to 6 ± 1 Å. We were particularly interested in identifying scaffolds with good pharmacological and toxicological properties, and accordingly,

a pharmacophore search was made in an in-house three-dimensional database of 1410 U.S. Food and Drug Administration (FDA) approved drugs. Eleven compounds were identified and were grouped into three classes on the basis of their scaffolds (Figure 3). Our initial efforts focused on the second class of compounds, which all contain the bis-aryl-substituted five-membered heterocyclic template and include the well-known drugs Lipitor and Celecoxib (Figure 3).

To explore the possible binding models of Lipitor and Celecoxib with Bcl-xL, we performed computational docking of both drugs to Bcl-xL using the crystal structure adopted by Bcl-xL in its complex with the BAD BH3 peptide. As can be seen in Figure 4A,B, the hydrophobic groups of Lipitor mimic Y105 and L109 of the BAD BH3 peptide in its interaction with Bcl-xL, whereas the two phenyl groups of Celecoxib mimic the interaction between L109 and M112 of the BAD BH3 peptide with Bcl-xL. Figure 4A,B suggested that the bis-aryl-substituted five-membered heterocycle scaffold could mimic two of three critical hydrophobic residues in the BAD BH3 peptide.

On the basis of these analyses, compound 4 (Figure 4C), containing a 3,4-diphenyl-1*H*-pyrrole-2-carboxamide scaffold, was designed. Since it was critical to determine the crystal structure of our initial lead compound complexed with Bcl-xL for subsequent optimization efforts, we have decided to attach two soluble groups in compound 4 to facilitate crystallographic studies. Docking studies suggested that compound 4 can effectively interact with the deep hydrophobic pocket in site 1.

Compound 4 was synthesized and evaluated for its binding to Bcl-xL and Bcl-2 proteins in fluorescence polarization (FP) assays. Compound 4 has K_i values of 78 μ M for Bcl-2 and 138 μ M for Bcl-xL (Table 1). Although in a typical drug discovery program such weak affinities would seem to disqualify it as a useful lead compound, it does possess an attractive druglike core structure and excellent aqueous solubility, and it was proven to be an excellent starting point in our design of new and potent Bcl-2/Bcl-xL inhibitors.

To provide a solid structural basis for our subsequent structure-based optimization of 4, we determined its crystal structure, at a resolution of 1.7 Å, in a complex with Bcl-xL (Figure 4D). This shows that 4 indeed binds to the large, deep hydrophobic pocket in site 1 of Bcl-xL, supporting both our modeling prediction and our design premise.

Structure-Based Design of Potent Bcl-2/Bcl-xL Inhibitors. For a compound to achieve a high binding affinity for Bcl-xL, it may be necessary to occupy both sites 1 and 2 in the protein.¹³ Since 4 occupies only site 1, a second fragment, capable of occupying site 2, is needed. We used the crystal structure of 1 complexed with Bcl-xL¹⁸ to identify a fragment that could be accommodated in site 2 (red circle in Figure 4D).

Superposition of the crystal structure of 4 and the crystal structure of 1 in its complex with Bcl-xL showed that the core structure in 4

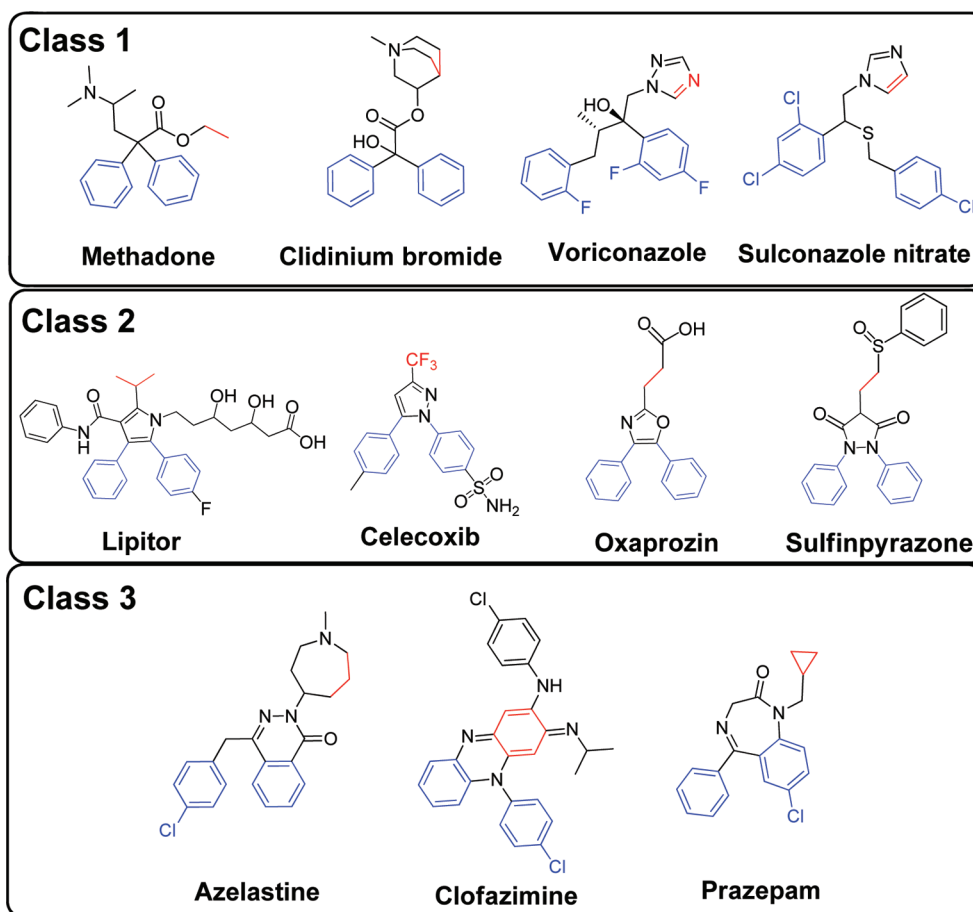


Figure 3. Three classes of scaffolds identified based on the pharmacophores in the Bad BH3 peptide. The three-dimensional pharmacophore model is based on two aromatic rings (shown in blue) and one hydrophobic group (shown in red). The distance between the aromatic rings was set to 5 ± 1 Å, and the distances between the aromatic ring and hydrophobic groups were set to 6 ± 1 Å.

and the *p*-chlorobiphenyl fragment in **1** (Figure 5A) both occupy site 1. It is also evident that fragment **5** occupies site 2 in Bcl-xL (Figure 5A,B). Therefore, we reasoned that linking compounds **4** and **5** could yield new compounds with high affinity for Bcl-xL.

Compound **5** was synthesized by the published method¹⁹ and found to have very weak affinities ($IC_{50} > 100 \mu M$) for Bcl-xL and Bcl-2 proteins in our FP-based assays. These data further showed that interacting with either site 1 or site 2 is insufficient to yield compounds with high affinities for Bcl-xL and Bcl-2, and occupation of both sites is needed to achieve high affinities for Bcl-xL and Bcl-2. Therefore, we decided to link **4** and **5** together with a proper linker for the design of potent inhibitors of Bcl-xL and Bcl-2.

Analysis of the modeled structure of **5** complexed with Bcl-xL and the crystal structures of **1** and **4** complexed with Bcl-xL suggested that the meta position of the unsubstituted phenyl ring in **4** and the sulfonamido nitrogen atom of **5** are sites at which **4** and **5** could be linked together for the design of potent Bcl-xL inhibitors (Figure 5B). The distance between this ring in **4** and the sulfonamido nitrogen atom of **5** is 8.2 Å (Figure 5B).

Compound **6**, designed to make use of the linker in **1** (Figures 5C and 6), which is 10.6 Å in length, was found to have $K_i = 2.0$ nM for Bcl-2 and $K_i < 1$ nM for Bcl-xL, and is thus >10 000 times more potent than either **4** or **5**. The dramatically improved binding affinities of **6** over those of **4** and **5** supported our design strategy.

Compounds **1** and **6** have similar affinities for Bcl-xL, but **6** is less potent than **1** toward Bcl-2 (Table 1). To further optimize the binding affinities of **6**, we next tested linkers with various

lengths, flexibility, orientation, and chemical properties (Figures 5C and 6). Modeling suggested that removal of the carbonyl group in the *N*-acylsulfonamide in **6** may lead to further improvement in the binding affinity (Figure S1 in Supporting Information). Removal of this carbonyl group from **6** gives **7**, in which the linker has been shortened from 10.6 to 9.9 Å. The affinity of **7** for both Bcl-2 and Bcl-xL ($K_i < 1$ nM) is very similar to that of **1**. Replacement of the piperazine in **7** by a triazole aromatic ring shortens the linker to 9.0 Å, giving **8**, which also binds to both Bcl-2 and Bcl-xL with $K_i < 1$ nM. Replacement of the piperazine ring in the linker in **6** with a rigid ethynyl group leads to **9**, which has a linker length of 9.1 Å and binds to both Bcl-2 and Bcl-xL with $K_i < 1$ nM. Removal of the carbonyl group from the *N*-acylsulfonamide group in **9** leads to **10**, which has a linker length of 8.3 Å and binds to Bcl-2 and Bcl-xL with $K_i = 1.5$ nM and 1.7 nM, respectively.

Hence, compounds **7**, **8**, and **9** bind to Bcl-2 and Bcl-xL with $K_i < 1$ nM and are as potent as **1** toward both proteins. The binding data show that tethering **4** and **5**, two weak Bcl-2/Bcl-xL inhibitors, with linkers approximately 9.0 Å in length produced highly potent Bcl-2/Bcl-xL inhibitors, whose affinities for Bcl-2/Bcl-xL are 4 orders of magnitude better than those of **4** or **5**. When the linker is longer (10.6 Å in **6**) or shorter (8.3 Å in **10**), the resulting compounds are less potent. To investigate the influence of linker flexibility, we synthesized **11**, with a more flexible linker than that in **7**, and found that **11** is at least 10 times less potent than **7**.

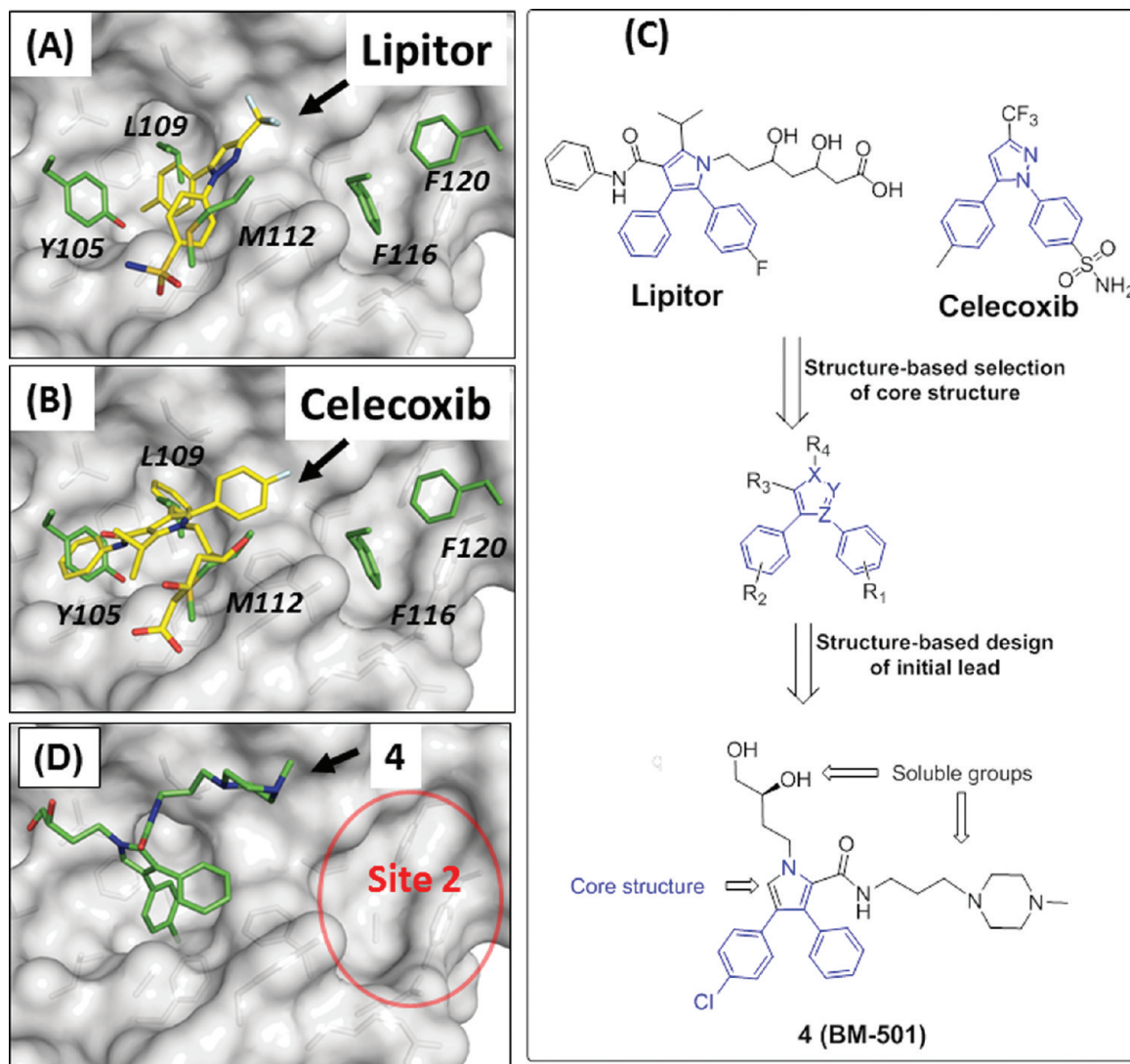


Figure 4. Structure-based design of a new scaffold as the initial lead compound **4** and its crystal structure in complex with Bcl-xL. (A, B) Rank 1 pose of (A) Lipitor and (B) Celecoxib with Bcl-xL, using the BAD BH3 peptide-bound Bcl-xL structure (PDB ID 2BZW). (C) Identification of the core scaffold from the FDA-approved drugs database for a new class of Bcl-2/Bcl-xL inhibitors. (D) Co-crystal structure of **4** in complex with Bcl-xL (1.7 Å).

Table 1. Binding Affinities of Our Designed Compounds for Bcl-2 and Bcl-xL Proteins in Fluorescence Polarization Assays and Inhibition of Cell Growth in Two Cancer Cell Lines

compd	binding affinities					cell growth inhibition, IC ₅₀ ± SD (μM)	
	Bcl-2 (FP)		Bcl-xL (FP)		Mcl-1	H146	H1417
	IC ₅₀ ± SD (nM)	K _i ± SD (nM)	IC ₅₀ ± SD (nM)	K _i ± SD (nM)	IC ₅₀ ± SD (μM)		
4	213 ± 16 (μM)	78.0 ± 5.9 (μM)	453 ± 25 (μM)	138 ± 7.6 (μM)	>100	>10	>10
5	>100 (μM)		238 ± 14 (μM)	75.0 ± 4.2 (μM)	>100	>10	>10
6	8.7 ± 1.9	2.0 ± 0.5	6.1 ± 1.5	<1	>10	>10	>10
7	1.3 ± 0.7	<0.6	6.2 ± 2.2	<1	>10	2.0 ± 1.1	1.8 ± 0.07
8	1.4 ± 0.8	<0.6	4.8 ± 1.1	<1	>10	>10	>10
9	1.9 ± 0.6	<0.6	5.7 ± 0.7	<1	>10	>10	>10
18	6.6 ± 2.2	1.5 ± 0.3	12.6 ± 3.1	1.7 ± 0.9	>10	>10	>10
19	60.6 ± 23.1	15.4 ± 6.0	44.1 ± 5.5	11.3 ± 0.6	>10	>10	>10
12	33.9 ± 3.8	8.5 ± 1.0	7.6 ± 1.6	<1	>10	2.5 ± 0.8	3.3 ± 1.4
13	85.3 ± 34.8	21.8 ± 9.0	88.3 ± 14.4	24.7 ± 4.0	>10	>10	>10
1	2 ± 0.2	<0.6	6 ± 2	<1	>1	0.097 ± 0.030	0.13 ± 0.05
14	>100 (μM)		547 (μM)	166 (μM)	>100	>10	>10
15	534 ± 105 (μM)	138 ± 27 (μM)	19 ± 0.3 (μM)	5.7 ± 0.1 (μM)	>100	>10 000	7.5 ± 0.7

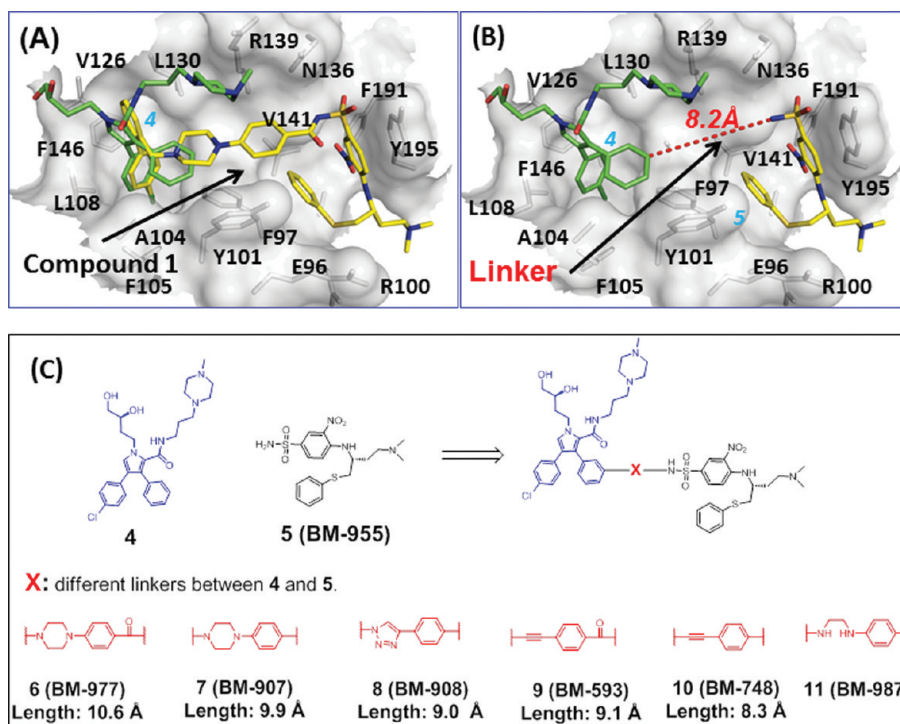


Figure 5. Computational structure-based design of a new class of Bcl-2/Bcl-xL inhibitors by linking two fragments with weak binding affinities. (A) Superposition of the crystal structure of **4** (green) onto the crystal structure of **1** (yellow) in complex with Bcl-xL (B) Measurement of the distance (8.2 Å) between **4** and **5**. The 1-bound Bcl-xL structure was used in the surface representation. (C) Chemical structures of **5** and the new designed Bcl-2/Bcl-xL inhibitors with different linkers.

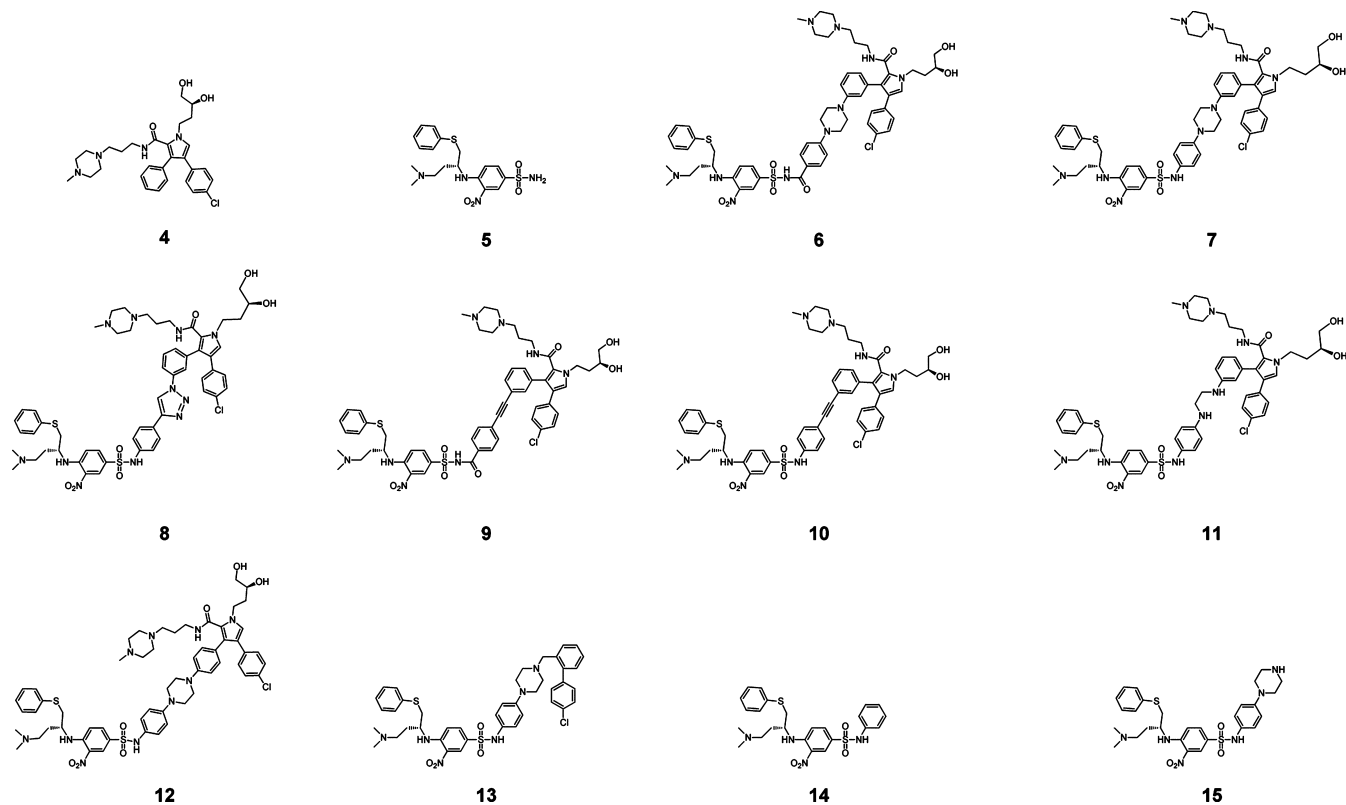


Figure 6. Chemical structures of designed Bcl-2 and Bcl-xL inhibitors.

To examine binding specificity, we evaluated the binding of these compounds to Mcl-1. Similar to **1**, compounds **6**, **7**, **8**, **9**, **10** and **11** all were found to bind to Mcl-1 with $IC_{50} > 10 \mu M$, thus showing very high specificity over Mcl-1 (Table 1).

Changing the attachment position of the linker from the meta to the para position of the phenyl ring in **7** results in **12** (Figure 6), which is >10 times less potent than **7** in binding to Bcl-2 but is equipotent with **7** in its binding to Bcl-xL (Table 1).

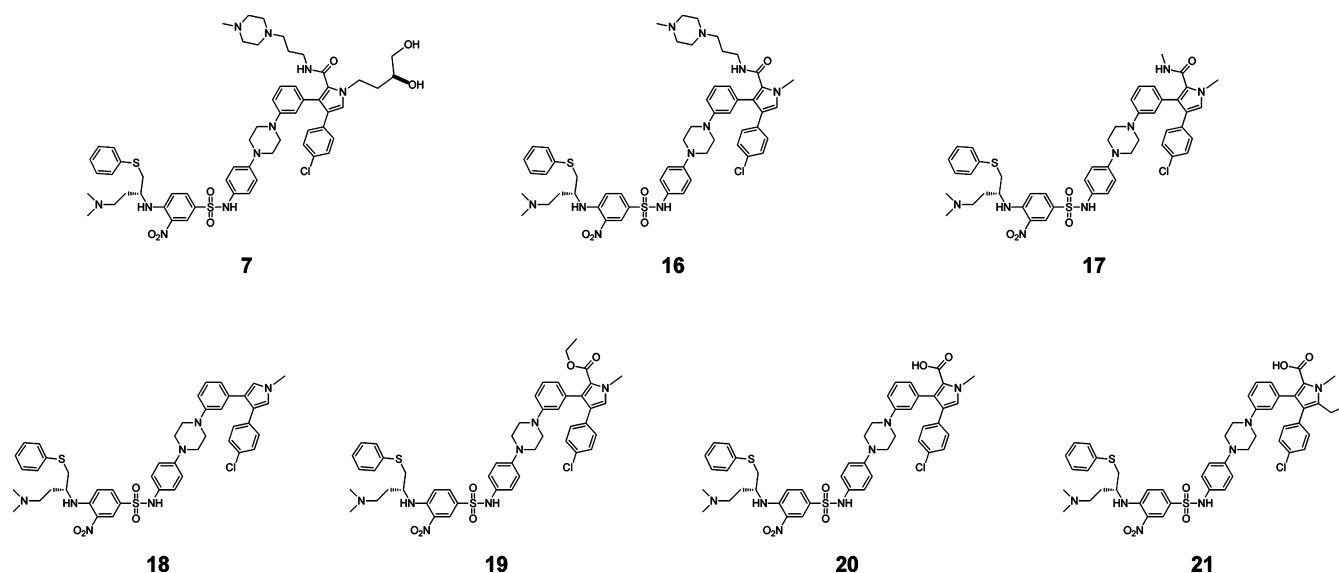


Figure 7. Chemical structures of 7 and its analogues.

Table 2. Binding Affinities of Our Designed Compounds for Bcl-2 and Bcl-xL Proteins in Fluorescence Polarization Assays and Inhibition of Cell Growth in Two Small-Cell Lung Cancer Cell Lines

compd	binding affinities					cell growth inhibition, $IC_{50} \pm SD$ (μM)	
	Bcl-2 (FP)		Bcl-xL (FP)		Mcl-1	H146	H1417
	$IC_{50} \pm SD$ (nM)	$K_i \pm SD$ (nM)	$IC_{50} \pm SD$ (nM)	$K_i \pm SD$ (nM)	$IC_{50} \pm SD$ (μM)		
7	1.3 \pm 0.7	<0.6	6.2 \pm 2.2	<1	>10	2.0 \pm 1.1	1.8 \pm 0.07
16	0.6 \pm 0.2	<0.6	4.9 \pm 1.2	<1	>10	0.43 \pm 0.25	0.65 \pm 0.51
17	5.3 \pm 0.6	1.2 \pm 0.2	6.3 \pm 0.4	<1	>2	0.40 \pm 0.31	0.65 \pm 0.15
18	82.6 \pm 19.5	21.1 \pm 5.0	34.4 \pm 3.5	8.3 \pm 1.0	>2	>10	>10
19	45.8 \pm 26.1	11.6 \pm 6.8	12.6 \pm 5.4	1.7 \pm 0.6	>2	4.9 \pm 3.2	7.3 \pm 2.8
20	1.7 \pm 1.0	<0.6	3.6 \pm 1.1	<1	>2	0.34 \pm 0.01	0.552 \pm 0.089
21	4.1 \pm 0.7	0.8 \pm 0.2	7.5 \pm 1.3	<1	>2	0.061 \pm 0.009	0.090 \pm 0.003
1	2 \pm 0.2	<0.6	6 \pm 2	<1	>1	0.097 \pm 0.03	0.13 \pm 0.05

We also synthesized 13 (Figure 6), an analogue of 1 lacking the benzamido carbonyl group. This compound binds to Bcl-2 and Bcl-xL with K_i values of 18 nM and 17 nM, respectively, an affinity >10 times weaker than that of 1. Hence, the carbonyl group in 1 evidently contributes significantly to its binding affinities for Bcl-2 and Bcl-xL. By contrast, removal of the corresponding carbonyl group in 6 enhances the binding affinity for Bcl-2 by 6 times while having no effect on the binding to Bcl-xL.

Compounds 14 and 15, fragments of 7 (Figure 6), were synthesized and their binding to Bcl-2 and Bcl-xL was examined. Both 14 and 15 bind to Bcl-2 and Bcl-xL with weak affinities (Table 1).

As a single agent, 1 was shown to be very effective in inhibition of cancer cell growth in cancer cell lines such as small-cell lung cancer cell lines H146 and H1417, with high levels of Bcl-2/Bcl-xL but low levels of Mcl-1. Since 7 and several other compounds bind to Bcl-2 and Bcl-xL with very high affinities, show high specificity over Mcl-1 and have the same binding profiles as 1, we evaluated their ability, in comparison to 1, to inhibit cell growth in the H146 and H1417 cancer cell lines with the results shown in Table 1.

Consistent with their weak binding affinities, four compounds (4, 5, 14, and 15) have poor activities ($IC_{50} > 10 \mu M$) in inhibition of cell growth in these two cancer cell lines. Although compounds 6, 8, 9, 10, and 11 all have high affinities for both Bcl-2 and Bcl-xL, they also have weak cellular activities ($IC_{50} > 10 \mu M$), suggesting that these compounds may suffer from poor cell per-

meability. Removal of the carbonyl group from the linker in 6 to give 7 significantly improves both the binding affinities for Bcl-2 and Bcl-xL and the cellular activity. Compound 7 inhibits cell growth in these two cancer cell lines and has IC_{50} values of approximately 2.0 μM against both cancer cell lines. In contrast, removal of the corresponding carbonyl group in 1, which results in compound 13, is detrimental to binding affinities for both Bcl-2 and Bcl-xL, as well as to the cell growth inhibitory activities. The binding and cellular data thus identify 7 as a promising lead compound for further optimization, and accordingly, we focused next on 7 to further investigate the structure–activity relationships (SAR) for this class of compounds.

Structure–Activity Relationships of Compound 7. Modeling suggested that the dihydroxybutyl side chain in 7 lacks any specific interactions with Bcl-xL (Figure S1B in Supporting Information). Removal of this dihydroxybutyl side chain yields 16 (Figure 7), which binds to Bcl-2 and Bcl-xL with $K_i < 1$ nM. It inhibits cell growth in the H146 and H1417 cancer cell lines with IC_{50} values of 0.43 μM and 0.65 μM , respectively, and is thus 3–5 times more potent than 7 (Table 2). The data thus show that truncation of the dihydroxybutyl side chain in 7 to a methyl group is accompanied by retention of the high binding affinities for Bcl-2/Bcl-xL and significant improvement in its cellular activities in both the H146 and H1417 cancer cell lines.

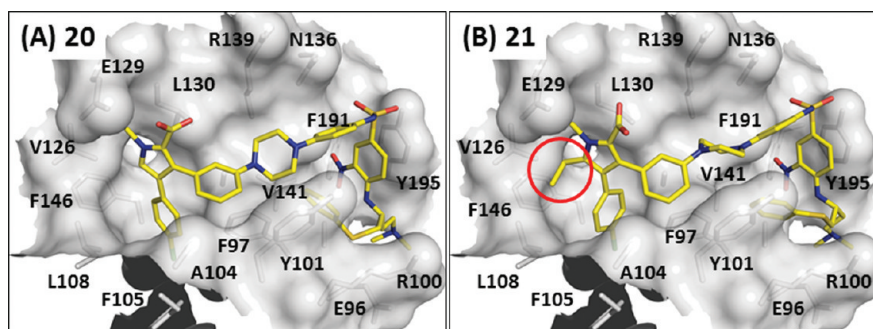


Figure 8. Binding models of (A) **20** and (B) **21** with Bcl-xL. The Bcl protein from the crystal structure between **1** and Bcl-xL was used in the docking simulations. The highest ranked poses of both compounds were selected as the binding models. The ethyl group added to **20** is denoted by the red circle. Residues of Bcl-xL at the binding site are labeled.

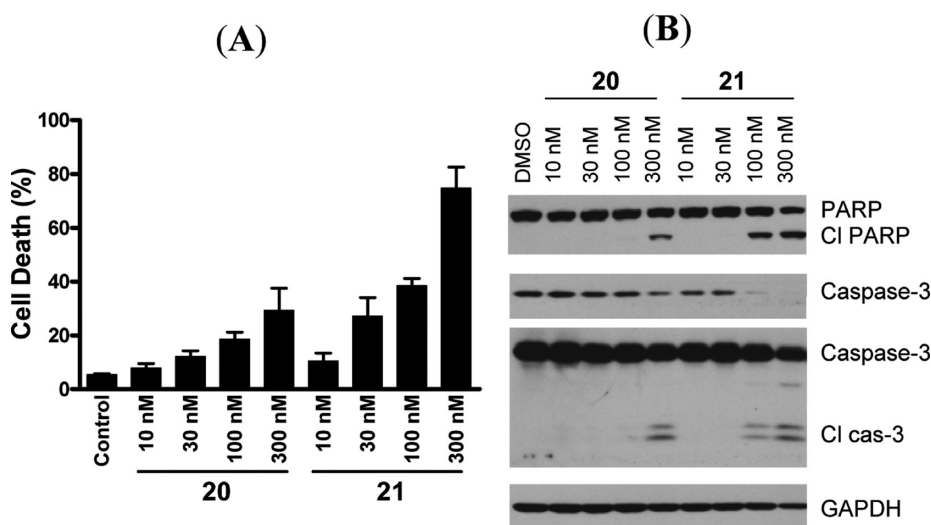


Figure 9. (A) Cell death induction by **20** and **21** in the H146 cancer cell line. Cells were treated for 24 h and cell death was analyzed by trypan blue assay. (B) Induction of cleavage of PARP and caspase-3 by **20** and **21** in the H146 cell line. Cells were treated for 24 h, and caspase-3 and PARP were probed by Western blotting.

The *N*-[3-(4-methylpiperazin-1-yl)propyl]amide side chain in **16** was used to improve the aqueous solubility. We investigated the effect of modifications of this side chain in **16** on binding to Bcl-2/Bcl-xL. Compound **17**, in which the *N*-[3-(4-methylpiperazin-1-yl)propyl]amide side chain in **16** was truncated to an *N*-methylcarbamoyl group (Figure 7), binds to Bcl-2 with $K_i = 1.2$ nM and to Bcl-xL with $K_i < 1$ nM. Compounds **16** and **17** thus have similar potencies in inhibition of cell growth against both the H146 and H1417 cell lines. Compound **18**, obtained by removal of the *N*-methylcarbamoyl group from **17**, has a much weaker binding affinity for both Bcl-2 and Bcl-xL than **16** and **17**. It also has very weak cellular activity in both H146 and H1417 cancer cell lines with IC_{50} values >10 μ M (Table 2). These data show that the amide group in **16** and **17** plays a role in binding to Bcl-2 and Bcl-xL and in inhibition of cell growth.

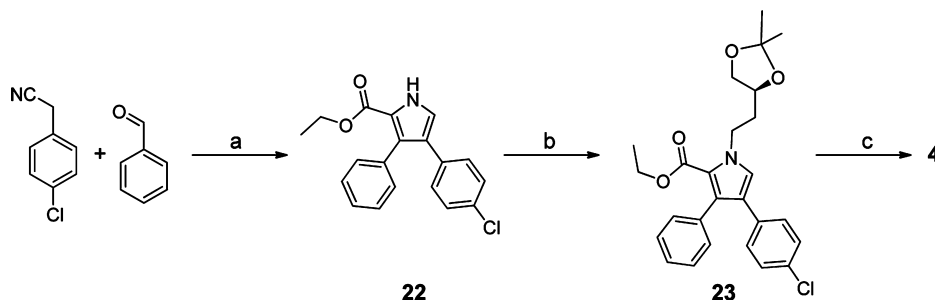
Replacement of the *N*-methylcarbamoyl substituent on the pyrrole ring in **17** by a carboxyl group results in **19** (Figure 7), which binds to Bcl-2 10 times less potently than **17**, but **19** is only slightly less potent than **17** in binding to Bcl-xL. It has IC_{50} values of 4.9 μ M and 7.3 μ M in inhibition of cell growth in H146 and H1417 cancer cell lines, respectively, and is thus 10 times less potent than **17** (Table 2).

Replacement of the *N*-methylcarbamoyl substituent on the pyrrole ring of **17** by a carboxyl substituent generates **20**, which

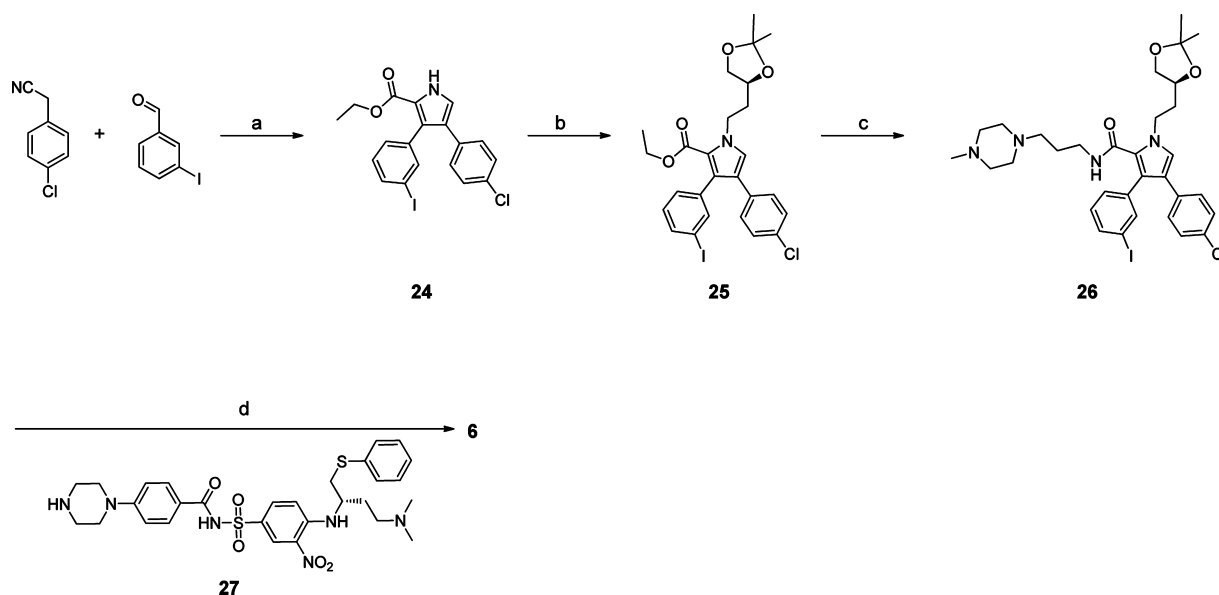
binds to Bcl-2 and Bcl-xL with high affinities, with $K_i < 1$ nM, and has IC_{50} values of 0.34 μ M and 0.55 μ M in inhibition of cell growth against the H146 and H1417 cancer cell lines, respectively.

In an effort to further improve the binding affinities and especially the cellular activity of **20**, we performed docking simulations of **20** based on the crystal structures of **4** and **1** complexed with Bcl-xL. The predicted binding model for **20** (Figure 8A) suggested that there is an unoccupied small hydrophobic pocket close to the 5-position of the pyrrole core in **20**. Accordingly, we designed and synthesized **21**, in which an additional ethyl group was introduced to the 5-position of the pyrrole ring in **20** (Figures 7 and 8B). Compound **21** binds to both Bcl-2 and Bcl-xL with very high affinities ($K_i < 1$ nM), actually exceeding the lower limits of the assays, and it has an improved cell-growth inhibitory activity against the H146 and H1417 cancer cell lines, with IC_{50} values of 61 nM and 90 nM, respectively. Hence, **21** is as potent as **1**, both in binding to Bcl-2 and Bcl-xL and in inhibition of cell growth against both the H146 and H1417 cancer cell lines.

Further Evaluation of Compounds 20 and 21. We next evaluated the ability of **20** and **21** to induce cell death in the H146 cell line (Figure 9A). Both compounds effectively induce cell death in a dose-dependent manner in H146 cells as

Scheme 1. Synthesis of Compound 4^a

^aReagents and conditions: (a) (i) K_2CO_3 , MeOH, reflux; (ii) $CNCH_2COOEt$, $t-BuOK$. (b) (*S*)-4-(2-Iodoethyl)-2,2-dimethyl-1,3-dioxolane, K_2CO_3 . (c) (i) KOH , $H_2O/THF/MeOH$; (ii) 3-(4-methylpiperazin-1-yl)propan-1-amine, EDCl, HOBt, DIEA, DCM; (iii) 4 M HCl in dioxane, MeOH.

Scheme 2. Synthesis of Compound 6^a

^aReagents and conditions: (a) (i) K_2CO_3 , MeOH, reflux; (ii) $CNCH_2COOEt$, $t-BuOK$. (b) (*S*)-4-(2-Iodoethyl)-2,2-dimethyl-1,3-dioxolane, K_2CO_3 . (c) (i) KOH , $H_2O/THF/MeOH$; (ii) 3-(4-methylpiperazin-1-yl)propan-1-amine, EDCl, HOBt, DIEA, DCM. (d) (i) 27, $Pd(dba)_2$, tri-*tert*-butylphosphine, sodium *tert*-butoxide, DMF, toluene; (ii) 4 M HCl in dioxane, MeOH, 10 min.

determined in a trypan blue assay, with **21** being more potent than **20**. Compound **21** induces substantial cell death at 30–100 nM and >70% cell death in 24 h at 300 nM.

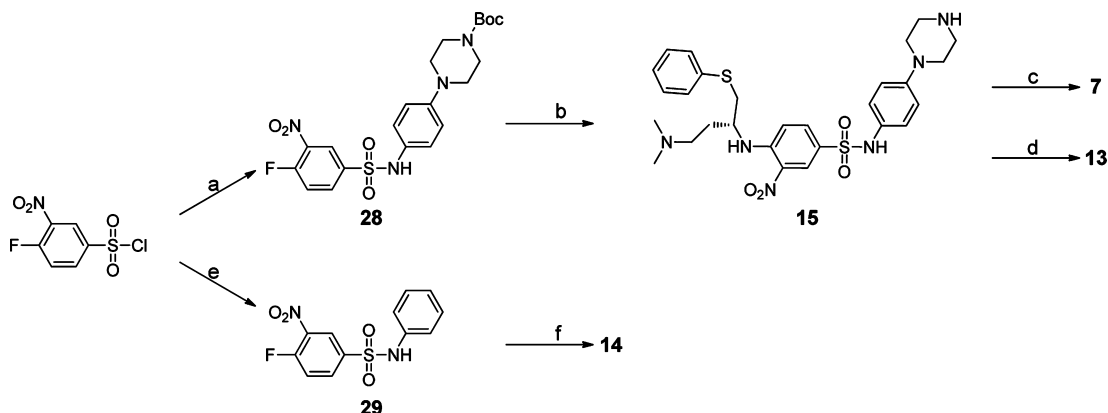
We further tested **20** and **21** in the H146 cell line for their ability to induce cleavage of poly(ADP-ribose) polymerase (PARP) and caspase-3, two biochemical markers of apoptosis (Figure 9B), and found that **21** is more potent than **20** and can effectively induce cleavage of PARP and caspase-3 in 24 h at concentrations as low as 100 nM. These data are consistent with their activities in the cell growth assay.

Synthesis. The synthesis of the initial lead compound (**4**) is outlined in Scheme 1. Briefly, benzaldehyde, 4-chlorophenyl cyanide, and K_2CO_3 were heated in methanol to generate 2-(4-chlorophenyl)-3-phenylacrylonitrile, which was used in a 2 + 3 cycloaddition reaction with ethyl isocyanoacetate to produce pyrrole **22**.²⁰ Alkylation of **22** with (*S*)-4-(2-iodoethyl)-2,2-dimethyl-1,3-dioxolane in the presence of K_2CO_3 at 60 °C in *N,N*-dimethylformamide (DMF) gave **23**, hydrolysis of which afforded the corresponding acid, which was coupled to 1-(3-amino-

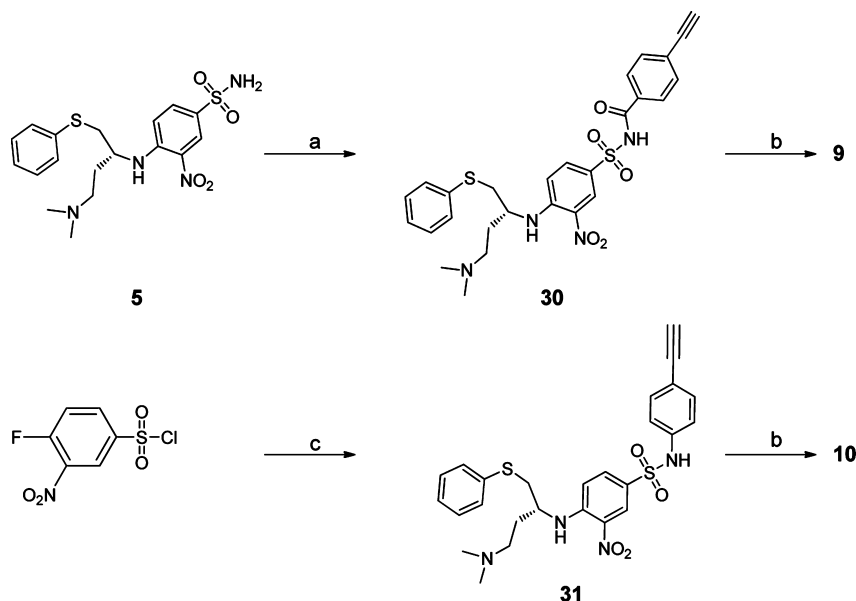
propyl)-4-methylpiperazine. Removal of the acetal protecting group with HCl produced **4**.

The synthesis of compound **6** is shown in Scheme 2. Compounds **24**, **25**, and **26** were synthesized, employing the same strategy as in Scheme 1, and intermediate **27** was prepared as described previously.¹⁹ Compound **6** was formed by palladium-catalyzed amination²¹ of **26** with **27** in the presence of $Pd(dba)_2$ and tri-*tert*-butylphosphine, followed by acetal deprotection.

Compounds **7**, **13**, **14**, and **15** were prepared as shown in Scheme 3. Commercially available 4-fluoro-3-nitrobenzene-1-sulfonyl chloride was treated with the corresponding aniline in pyridine at 0 °C to produce the sulfonamides **28** and **29**. (*R*)-*N*¹,*N*¹-dimethyl-4-(phenylthio)butane-1,3-diamine was used to displace the fluorine in **28** and the Boc group was removed to give compound **15**. Using the same strategy, **14** was synthesized from **29**. Palladium-catalyzed amination was again employed to couple **15** and **26**, and the resulting compound was deprotected to generate compound **7**. Reductive amination of **15** with 4'-chloro-[1, 1'-biphenyl]-2-carbaldehyde was employed in the

Scheme 3. Synthesis of Compounds 7, 13, 14, and 15^a

^aReagents and conditions: (a) *tert*-Butyl 4-(4-aminophenyl)piperazine-1-carboxylate, pyridine. (b) (i) (*R*)-*N*¹,*N*¹-Dimethyl-4-(phenylthio)butane-1,3-diamine, DIEA, DMF; (ii) TFA, CH₂Cl₂. (c) (i) **26**, Pd(dba)₂, tri-*tert*-butylphosphine, sodium *tert*-butoxide, DMF, toluene; (ii) 4 M HCl in dioxane, MeOH, 10 min. (d) 4'-Chloro-[1,1'-biphenyl]-2-carbaldehyde, Na(OAc)₃BH, ClCH₂CH₂Cl. (e) Aniline, pyridine. (f) (*R*)-*N*¹,*N*¹-Dimethyl-4-(phenylthio)butane-1,3-diamine, DIEA, DMF.

Scheme 4. Synthesis of Compounds 9 and 10^a

^aReagents and conditions: (a) 4-Ethynylbenzoic acid, EDCI, DMAP, CH₂Cl₂. (b) (i) **26**, Pd(PPh₃)₄, CuI, Et₃N, DMF; (ii) 4 M HCl in dioxane, MeOH, 10 min. (c) (i) 4-Ethynylaniline, pyridine; (ii) (*R*)-*N*₁,*N*₁-dimethyl-4-(phenylthio)butane-1,3-diamine, DIPEA, DMF.

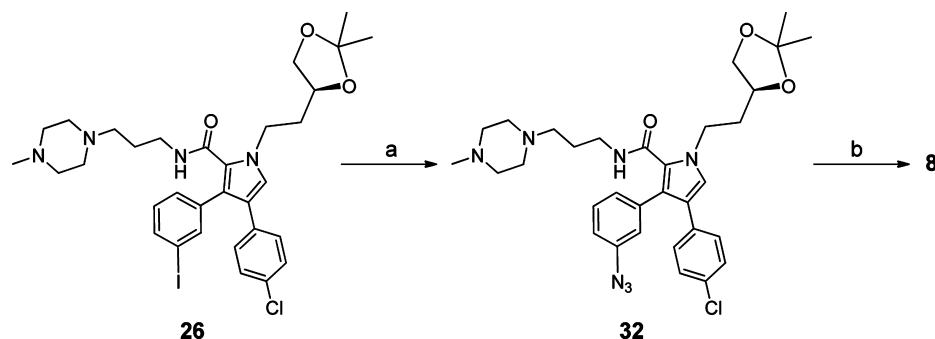
presence of sodium triacetoxyborohydride and 1,2-dichloroethane to give **13**.

Compounds **9** and **10**, in which the linker is an ethynyl group, were synthesized as shown in Scheme 4. Compound **5** was synthesized by the published procedure.¹⁹ Compound **5** was then coupled with 4-ethynylbenzoic acid in the presence of 1-ethyl-3-[3-(dimethylamino)propyl]carbodiimide (EDCI) to give compound **30**. Pd(0)-catalyzed coupling²² of the iodide **26** with the terminal alkyne **30**, followed by deprotection of the acetal with HCl, yielded compound **9**. Compound **10** was synthesized by a procedure similar to that for compound **9**.

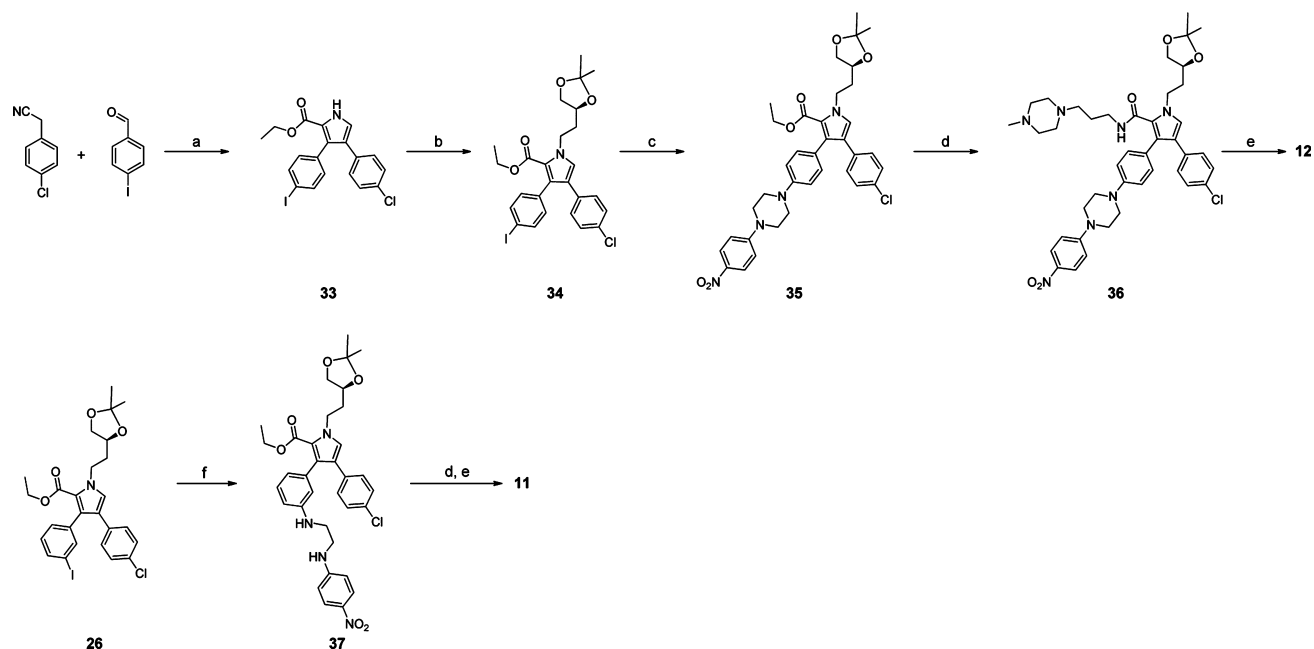
Scheme 5 shows synthesis of compound **8** with a triazole ring as the linker. CuI/*L*-proline-catalyzed coupling reaction²³ of aryl iodide **26** with sodium azide was carried out at 70 °C in dimethyl sulfoxide (DMSO) to produce **32**. This aryl azide **32** and alkyne **31** were joined by a Cu^I-catalyzed Huisgen cyclo-

addition²⁴ in a mixture of water and *t*-butanol in the presence of CuSO₄·5H₂O and (+)-sodium *L*-ascorbate. The acetal group in the resulting triazole was removed with HCl to produce compound **8**.

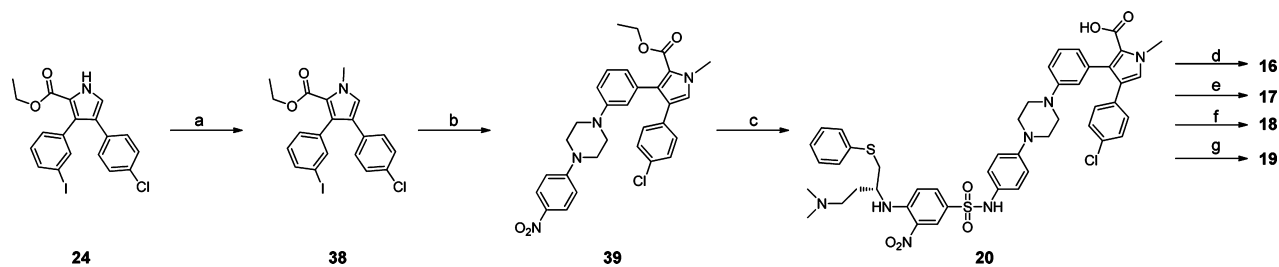
The linear synthetic strategy shown in Scheme 6 was employed to prepare compounds **12** and **11**. Compounds **33** and **34** were synthesized by the strategy described in Scheme 1. With *L*-proline as a promotor, Ullmann-type C–N bond formation reaction²⁵ of **34** with 1-(*p*-nitrophenyl)piperazine provided intermediate **35**, and subsequent hydrolysis of the ethyl ester and coupling with 1-(3-aminopropyl)-4-methylpiperazine in the presence of EDCI gave **36**. Hydrogenation of the nitro group in **36** gave the aniline, which was treated with 4-fluoro-3-nitrobenzene-1-sulfonyl chloride in pyridine. Subsequent displacement of the fluoro group with (*R*)-*N*¹,*N*¹-dimethyl-4-(phenylthio)butane-1,3-diamine and acetal deprotection

Scheme 5. Synthesis of Compound 8^a

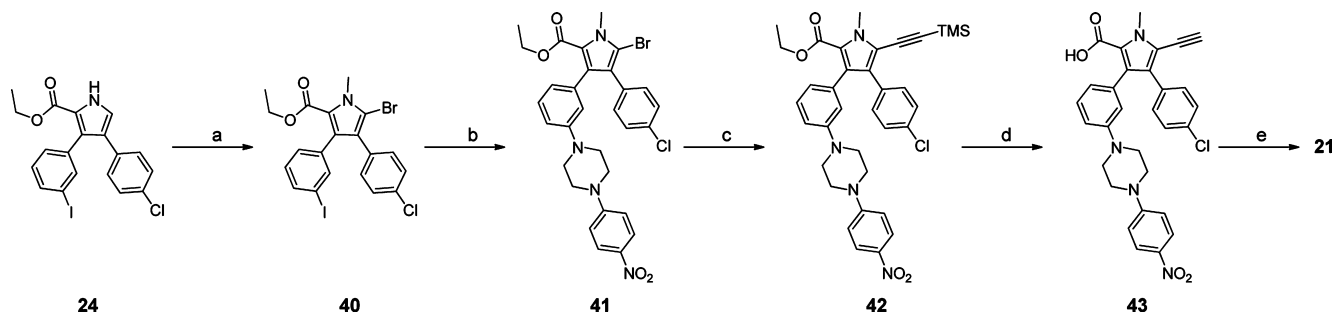
^aReagents and conditions: (a) NaN_3 , CuI , *L*-proline, NaOH , DMSO , 70°C . (b) (i) **31**, $\text{CuSO}_4 \cdot 5\text{H}_2\text{O}$, sodium *L*-ascorbate, $\text{H}_2\text{O}/t\text{-BuOH}$; (ii) 4 M HCl in dioxane, MeOH , 10 min.

Scheme 6. Synthesis of Compounds 12 and 11^a

^aReagents and conditions: (a) (i) K_2CO_3 , MeOH , reflux; (ii) $\text{CNCH}_2\text{COOEt}$, $t\text{-BuOK}$. (b) (*S*)-(2-iodoethyl)-2,2-dimethyl-1,3-dioxolane, K_2CO_3 . (c) 1-(4-Nitrophenyl)piperazine, CuI , *L*-proline, K_2CO_3 , 80°C , 2 h. (d) (i) KOH , $\text{H}_2\text{O}/\text{THF}/\text{MeOH}$; (ii) 3-(4-methylpiperazin-1-yl)propan-1-amine, EDCI , HOBT , DIEA , DCM . (e) (i) H_2 , Pd/C ; (ii) 4-fluoro-3-nitrobenzene-1-sulfonyl chloride, pyridine; (iii) (*R*)- N^1,N^1 -dimethyl-4-(phenylthio)butane-1,3-diamine, DIPEA , DMF . (iv) 4 M HCl in dioxane, MeOH . (f) N^1 -(4-Nitrophenyl)ethane-1,2-diamine, CuI , *L*-proline, K_2CO_3 , 80°C , overnight.

Scheme 7. Synthesis of Compounds 16–20^a

^aReagents and conditions: (a) MeI , K_2CO_3 . (b) 1-(4-Nitrophenyl)piperazine, CuI , *L*-proline, K_2CO_3 , 80°C , 2 h. (c) (i) KOH , $\text{H}_2\text{O}/\text{THF}/\text{MeOH}$, reflux; (ii) H_2 , Pd/C ; (iii) 4-fluoro-3-nitrobenzene-1-sulfonyl chloride, pyridine; (iv) (*R*)- N^1,N^1 -dimethyl-4-(phenylthio)butane-1,3-diamine, DIPEA , DMF . (d) 3-(4-Methylpiperazin-1-yl)propan-1-amine, EDCI , HOBT , DIEA , DCM . (e) Methylamine, EDCI , HOBT , DIEA , DCM . (f) TFA , CH_2Cl_2 . (g) EtOH , N,N' -diisopropylcarbodiimide, 4-(dimethylamino)pyridine, THF .

Scheme 8. Synthesis of Compound 21^a

^aReagents and conditions: (a) (i) NBS, DMF; (ii) MeI, K₂CO₃. (b) 1-(4-Nitrophenyl)piperazine, CuI, L-proline, K₂CO₃, 80 °C, 2 h. (c) Ethynyltrimethylsilane, Pd(PPh₃)₄, CuI, Et₃N, DMF, 85 °C. (d) KOH, dioxane, EtOH, H₂O, reflux, 2 h. (e) (i) H₂, Pd/C; (ii) 4-fluoro-3-nitrobenzene-1-sulfonyl chloride, pyridine; (iii) (*R*)-*N*¹,*N*¹-dimethyl-4-(phenylthio)butane-1,3-diamine, DIPEA, DMF.

with HCl produced 12. Compound 11 was synthesized similarly.

The syntheses of compounds 16–20 are outlined in Scheme 7. Methylation with MeI and subsequent Ullmann-type C–N bond formation reaction of 24 yielded compound 39. Compound 20 was prepared from 39 by a strategy similar to that used for 12. The amides 16 and 17 were produced by coupling the acid 20 to the corresponding amines by use of EDCI and hydroxybenzotriazole (HOBT). Treatment of 20 with trifluoroacetic acid (TFA) afforded the decarboxylated compound 18. The ester 19 was synthesized by condensation of ethanol and the acid 20 with *N,N*-diisopropylcarbodiimide in the presence of 4-(dimethylamino)pyridine.

Compound 21 was prepared as shown in Scheme 8. Bromination of 24 with *N*-bromosuccinimide (NBS) in DMF and subsequent methylation afforded 40, which was coupled to 1-(*p*-nitrophenyl)piperazine to give the intermediate 41. Sonogashira coupling of 41 with ethynyltrimethylsilane in the presence of CuI and Pd(PPh₃)₄ yielded 42. Hydrolysis of the ethyl ester and simultaneous removal of the trimethylsilane protecting group in 42 afforded 43. Reduction of the nitro and ethynyl groups in 43 with H₂ and Pd/C as the catalyst gave a product which, subjected to the same strategy as described in Scheme 7, yielded compound 21.

SUMMARY

Employing a computational structure-based design strategy, we have designed compound 4, which contains a novel druglike scaffold and binds to one well-defined binding pocket in Bcl-xL. The binding model of 4 with Bcl-xL was determined experimentally by X-ray crystallography. On the basis of the crystal structure of 4 and of 1 (ABT-737) in complex with Bcl-xL, we employed 4 and 5, a large fragment of 1, for the design of new small-molecule inhibitors that occupy two separate binding pockets in Bcl-xL. Although both 4 and 5 bind to Bcl-2 and Bcl-xL with very weak affinities, linking them together with appropriate linkers yielded compounds with very high affinities ($K_i < 1$ nM) for both Bcl-2 and Bcl-xL. Optimization of the linker between them resulted in 7, which not only binds to Bcl-2 and Bcl-xL with high affinities ($K_i < 1$ nM) but also potently inhibits cell growth in two small-cell lung cancer cell lines, which are sensitive to potent and specific Bcl-2/Bcl-xL inhibitors. Our results demonstrate that linking two molecules with very weak affinities for Bcl-2/Bcl-xL with appropriate linkers can result in highly potent Bcl-2/Bcl-xL inhibitors.

The nature of the linker plays a key role in achieving high binding affinities for Bcl-2/Bcl-xL and potent cell growth inhibitory activity against cancer cells. Further structure–activity relationship studies of 7 yielded a very promising lead compound, 21, which binds to Bcl-2 and Bcl-xL with K_i values < 1 nM, exceeding the limits of the binding assays. Compound 21 achieves IC₅₀ values of 60 and 90 nM against the H146 and H1417 cancer cell lines and induces robust cell death in the H146 cancer cell line at 30 nM. It is now the subject of further optimization, the results of which will be reported in future publications.

EXPERIMENTAL SECTION

General Chemistry Information. Unless otherwise stated, all reactions were performed under nitrogen atmosphere in dry solvents under anhydrous conditions. Reagents were used as supplied without further purification unless otherwise noted. NMR spectra were acquired at a proton frequency of 300 MHz, and chemical shifts are reported in parts per million (ppm) relative to an internal standard. The final products were purified by a C18 reverse phase semipreparative HPLC column with solvent A (0.1% TFA in water) and solvent B (0.1% TFA in CH₃CN) as eluents.

Ethyl 4-(4-Chlorophenyl)-3-phenyl-1*H*-pyrrole-2-carboxylate (22). A mixture of benzaldehyde (1.06 g, 10 mmol), 4-chlorophenyl cyanide (1.52 g, 10 mmol), and K₂CO₃ (1.66 g, 12 mmol) was refluxed overnight in MeOH (15 mL) under N₂. The mixture was cooled, poured into H₂O (15 mL), and stirred for 20 min. The precipitate was collected by filtration, washed with H₂O (2 × 15 mL) and petroleum ether (2 × 15 mL), and air-dried to give 2-(4-chlorophenyl)-3-phenylacrylonitrile. A solution of this compound and ethyl isocyanoacetate (1.13 g, 10 mmol) in tetrahydrofuran (THF; 20 mL) was added dropwise to a stirred solution of potassium *t*-butoxide (1.34 g, 12 mmol) in DMF (15 mL) at 0 °C under N₂. After being stirred at 0 °C for 1 h, the reaction mixture was diluted with H₂O (20 mL) and extracted with EtOAc (2 × 20 mL). The combined organic fractions were washed with water (20 mL) and then with brine (20 mL). After removal of the solvent under vacuum, the residue was purified by flash chromatography on silica gel to afford 22 (1.7 g, 52% over two steps). ¹H NMR (300 MHz, CCl₃D) δ 9.62 (br s, 1H), 7.32–7.30 (m, 5H), 7.18 (d, *J* = 8.3 Hz, 2H), 7.11 (d, *J* = 2.9 Hz, 1H), 7.05 (d, *J* = 8.3 Hz, 2H), 4.22 (q, *J* = 7.1 Hz, 2H), 1.16 (t, *J* = 7.1 Hz, 3H); ¹³C NMR (75 MHz, CCl₃D) δ 161.4, 134.2, 133.1,

131.9, 130.8, 129.5, 129.2, 128.4, 127.6, 127.0, 125.5, 120.4, 120.2, 60.4, 14.0.

(S)-Ethyl 4-(4-Chlorophenyl)-1-[2-(2,2-dimethyl-1,3-dioxolan-4-yl)ethyl]-3-phenyl-1H-pyrrole-2-carboxylate (23). Compound **22** (1.7 g 5.2 mmol), (S)-4-(2-iodoethyl)-2,2-dimethyl-1,3-dioxolane (2.0 g, 7.8 mmol), and K_2CO_3 (2.2 g, 15.6 mmol) in DMF (15 mL) were heated to 60 °C for 8 h. The reaction was cooled, diluted with water (20 mL), and extracted into EtOAc (30 mL, 2 × 20 mL). The combined organic fractions were washed with water (4 × 10 mL) and then with brine (10 mL) and dried over Na_2SO_4 . After evaporation of the solvent, the residue was purified by flash chromatography on silica gel to provide **23** (2.2 g, 92% yield). 1H NMR (300 MHz, CCl_3D) δ 7.30–7.28 (m, 3H), 7.21–7.18 (m, 2H), 7.13 (d, J = 8.5 Hz, 2H), 7.07 (s, 1H), 6.99 (d, J = 8.5 Hz, 2H), 4.65–4.57 (m, 1H), 4.47–4.38 (m, 1H), 4.17–4.01 (m, 4H), 3.61 (t, J = 7.3 Hz, 1H), 2.23–2.15 (m, 1H), 2.09–1.98 (m, 1H), 1.48 (s, 3H), 1.39 (s, 3H), 0.93 (t, J = 7.1 Hz, 3H); ^{13}C NMR (75 MHz, CCl_3D) δ 161.5, 135.8, 133.0, 131.6, 131.4, 130.6, 129.2, 128.3, 127.6, 126.7, 126.3, 123.0, 119.9, 73.2, 69.1, 59.8, 46.8, 35.5, 27.1, 25.7, 13.6.

(S)-4-(4-Chlorophenyl)-1-(3,4-dihydroxybutyl)-N-[3-(4-methylpiperazin-1-yl)propyl]-3-phenyl-1H-pyrrole-2-carboxamide (4). Potassium hydroxide (0.2 g, 3.6 mmol) was added to a solution of **23** (0.54 g, 1.2 mmol) in a mixture of THF/methanol/water (1:1:1, 10 mL) and the solution was refluxed until no starting material could be detected by thin-layer chromatography (TLC). After being cooled, the reaction was neutralized with 1 M HCl and extracted with EtOAc. The EtOAc solution was washed with brine, dried over Na_2SO_4 , and concentrated in vacuum to produce the crude acid, which was used in the next step without purification. A solution of this acid, 1-(3-aminopropyl)-4-methylpiperazine (0.23 g, 1.4 mmol), EDCI (0.35 g 1.8 mmol), HOBt (0.23 g, 1.8 mmol), and *N,N*-diisopropylethylamine (0.42 mL, 2.4 mmol) in dichloromethane (DCM; 10 mL) was stirred for 8 h and then concentrated. The residue was resolved in MeOH (10 mL) and treated with 1 mL of HCl solution (4 N in dioxane) for 10 min, and then the solvent was removed under vacuum. The residue was then purified by HPLC to provide **4** (0.5 g, 79%). 1H NMR (300 MHz, CD_3OD) δ 7.24–7.20 (m, 3H), 7.09–6.89 (m, 5H), 6.88 (d, J = 8.5 Hz, 2H), 4.28–4.16 (m, 2H), 3.50–3.35 (m, 11H), 3.12–3.04 (m, 2H), 2.85 (s, 3H), 2.82–2.75 (m, 2H), 1.95–1.89 (m, 1H), 1.68–1.63 (m, 3H); ^{13}C NMR (75 MHz, CD_3OD) δ 165.6, 136.2, 134.9, 132.6, 131.8, 130.5, 129.7, 129.2, 128.4, 126.6, 126.1, 124.9, 123.6, 70.2, 67.3, 55.5, 51.6, 49.9, 46.2, 43.4, 37.3, 36.4, 25.1; ESI MS m/z 525.8 (M + H)⁺.

Ethyl 4-(4-Chlorophenyl)-3-(3-iodophenyl)-1H-pyrrole-2-carboxylate (24). Compound **24** was prepared by a procedure similar to that used for compound **22**. The yield was 49% in two steps. 1H NMR (300 MHz, CCl_3D) δ 9.48 (s, 1H), 7.74 (s, 1H), 7.64 (d, J = 7.8 Hz, 1H), 7.20 (d, J = 8.4 Hz, 2H), 7.14 (d, J = 7.7 Hz, 1H), 7.10 (d, J = 2.9 Hz, 1H), 7.05–7.00 (m, 3H), 4.22 (q, J = 7.1 Hz, 2H), 1.20 (t, J = 7.1 Hz, 3H); ^{13}C NMR (75 MHz, CCl_3D) δ 161.2, 139.7, 136.4, 135.9, 132.6, 132.2, 130.0, 129.5, 129.3, 128.5, 127.1, 125.5, 120.42, 120.39, 93.3, 60.6, 14.1.

(S)-Ethyl 4-(4-Chlorophenyl)-1-[2-(2,2-dimethyl-1,3-dioxolan-4-yl)ethyl]-3-(3-iodophenyl)-1H-pyrrole-2-carboxylate (25). Compound **25** was prepared in 87% yield from **24** by a procedure similar to that used with compound **23**. 1H NMR (300 MHz, CCl_3D) δ 7.67 (s, 1H), 7.62 (d, J = 7.8 Hz,

1H), 7.16 (d, J = 8.5 Hz, 2H), 7.10–6.97 (m, 5H), 4.63–4.56 (m, 1H), 4.46–4.39 (m, 1H), 4.15–4.03 (m, 4H), 3.60 (t, J = 6.7 Hz, 1H), 2.21–2.14 (m, 1H), 2.07–1.99 (m, 1H), 1.47 (s, 3H), 1.38 (s, 3H), 1.00 (t, J = 7.1 Hz, 3H); ^{13}C NMR (75 MHz, CCl_3D) δ 161.2, 139.7, 138.1, 135.6, 132.6, 131.9, 129.7, 129.4, 129.3, 128.4, 126.5, 123.0, 119.9, 93.3, 73.1, 69.1, 60.0, 46.8, 35.5, 27.1, 25.7, 13.8; ESI MS m/z 580.1 (M + H)⁺.

(S)-4-(4-Chlorophenyl)-1-[2-(2,2-dimethyl-1,3-dioxolan-4-yl)ethyl]-3-(3-iodophenyl)-N-[3-(4-methylpiperazin-1-yl)propyl]-1H-pyrrole-2-carboxamide (26). Potassium hydroxide (0.71 g, 12.6 mmol) was added to a solution of **25** (2.44 g, 4.2 mmol) in a mixture of THF/MeOH/ H_2O (1:1:1, 30 mL) and the solution was refluxed until no starting material was detectable by TLC. After being cooled, the reaction was neutralized with 1 M HCl and the compound was extracted with EtOAc. The EtOAc solution was washed with brine, dried over Na_2SO_4 , and concentrated in vacuum to produce the crude acid, which was used directly in the next step without purification. A solution of this acid, 1-(3-aminopropyl)-4-methylpiperazine (0.86 g, 5.5 mmol), EDCI (1.5 g 6.3 mmol), HOBt (1.0 g, 6.3 mol), and *N,N*-diisopropylethylamine (1.46 mL, 8.4 mmol) in DCM (15 mL) was stirred for 8 h and then concentrated. The residue was purified by flash chromatography on silica gel to afford **26** (2.26 g, 78% in two steps). 1H NMR (300 MHz, CCl_3D) δ 7.66–7.64 (m, 2H), 7.16–7.13 (m, 3H), 7.05 (t, J = 7.8 Hz, 1H), 6.95–6.93 (m, 3H), 5.59 (t, J = 5.1 Hz, 1H), 4.47–4.43 (m, 1H), 4.38–4.31 (m, 1H), 4.11–4.00 (m, 2H), 3.55 (t, J = 7.1 Hz, 1H), 3.26–3.19 (m, 2H), 2.35–1.97 (m, 15H), 1.49–1.43 (m, 5H), 1.34 (s, 3H); ^{13}C NMR (75 MHz, CCl_3D) δ 161.5, 139.3, 137.0, 136.5, 132.8, 131.8, 130.4, 129.9, 129.2, 128.4, 124.3, 124.1, 123.1, 122.1, 94.6, 73.2, 69.1, 55.8, 55.0, 53.0, 46.2, 46.0, 38.0, 35.7, 27.0, 26.1, 25.7; ESI MS m/z 691.6 (M + H)⁺.

4-(4-Chlorophenyl)-1-[(S)-3,4-dihydroxybutyl]-3-[3-(4-[[4-[[4-[(S)-4-(dimethylamino)-1-(phenylthio)but-2-yl]-amino]-3-nitrophenyl)sulfonyl]carbonyl]phenyl]piperazin-1-yl]phenyl]-N-[3-(4-methylpiperazin-1-yl)propyl]-1H-pyrrole-2-carboxamide (6). $Pd(dba)_2$ (3.5 mg, 0.006 mmol), tri-*tert*-butylphosphine (1 M in toluene, 4.8 μ L), and sodium *tert*-butoxide (18 mg, 0.18 mmol) were added to a stirred slurry of **26** (83 mg, 0.12 mmol) and **27** (88 mg, 0.14 mmol) in a mixture of toluene/DMF (1:1, 4 mL) at room temperature under N_2 . The mixture was heated to 70 °C and monitored by thin-layer chromatography. After complete consumption of starting materials, the reaction mixture was filtered through Celite and concentrated. The residue was resolved in MeOH (5 mL) and treated with 0.2 mL of HCl solution (4 M in dioxane) for 10 min, and then the solvent was removed in vacuum. Purification of the residue by HPLC afforded **6** (39 mg, 29%). 1H NMR (300 MHz, CD_3OD) δ 8.66 (d, J = 2.2 Hz, 1H), 7.93 (dd, J = 2.2, 9.2 Hz, 1H), 7.75 (d, J = 9.0 Hz, 2H), 7.29–6.95 (m, 15H), 6.81 (s, 1H), 6.74 (d, J = 7.4 Hz, 1H), 4.38–4.27 (m, 2H), 4.16–4.13 (m, 1H), 3.54–3.32 (m, 11H), 3.24–3.08 (m, 14H), 2.84 (s, 6H), 2.82 (s, 3H), 2.61 (t, J = 7.1 Hz, 2H), 2.27–2.14 (m, 2H), 2.03–2.00 (m, 1H), 1.78–1.75 (m, 1H), 1.66–1.61 (m, 2H); ^{13}C NMR (75 MHz, CD_3OD) δ 167.2, 165.4, 155.8, 152.1, 148.5, 137.2, 136.2, 135.6, 135.0, 132.5, 132.2, 131.5, 130.6, 130.4, 130.1, 129.7, 127.8, 127.5, 126.8, 126.0, 124.9, 123.7, 123.5, 121.7, 119.7, 116.5, 115.7, 114.8, 70.2, 67.3, 55.9, 55.4, 53.0, 52.4, 50.7, 50.2, 48.0, 46.2, 43.6, 43.5, 39.3, 37.6, 36.4, 30.1, 25.9; ESI MS m/z 1135.6 (M + H)⁺.

***t*-Butyl 4-[4-(4-Fluoro-3-nitrophenylsulfonamido)phenyl]piperazine-1-carboxylate (28).** 4-Fluoro-3-nitrobenzene-1-sulfonyl chloride (312 mg, 1.3 mmol) was added to *t*-butyl 4-(4-aminophenyl)piperazine-1-carboxylate (360 mg, 1.3 mmol) in pyridine (10 mL) at 0 °C. The mixture was stirred at 0 °C for 30 min and then concentrated under vacuum. The residue was purified by flash chromatography on silica gel to afford **28** (474 mg, 76%). ¹H NMR (300 MHz, CCl₃D) δ 8.43 (dd, *J* = 2.2, 6.8 Hz, 1H), 7.95–7.90 (m, 1H), 7.37 (t, *J* = 9.3 Hz, 1H), 7.01–6.98 (m, 3H), 6.81 (d, *J* = 8.9 Hz, 2H), 3.59–3.56 (m, 4H), 3.13–3.10 (m, 4H), 1.49 (s, 9H); ESI MS *m/z* 480.9 (M + H)⁺.

(*R*)-4-[[4-(Dimethylamino)-1-(phenylthio)but-2-yl]amino]-3-nitro-*N*-[4-(piperazin-1-yl)phenyl]benzenesulfonamide (15). DIEA (70 μL, 0.4 mmol) was added to a solution of **28** (100 mg, 0.21 mmol) and (*R*)-*N*¹,*N*¹-dimethyl-4-phenylthio)butane-1,3-diamine (47 mg, 0.21 mmol) in DMF. The solution was stirred overnight and then concentrated. The residue was resolved in MeOH (5 mL) and treated with HCl solution (4 M in dioxane, 4 mL), which was stirred for 5 h and then concentrated. This residue was purified by HPLC to afford **15** (170 mg, 81% over two steps). ¹H NMR (300 MHz, CD₃OD) δ 8.24 (d, *J* = 2.2 Hz, 1H), 7.56 (dd, *J* = 2.2, 9.1 Hz, 1H), 7.13–7.10 (m, 2H), 7.04–6.87 (m, 8H), 4.09–4.07 (m, 1H), 3.37–3.27 (m, 10H), 3.21–3.13 (m, 2H), 2.82 (s, 6H), 2.24–2.14 (m, 2H); ¹³C NMR (75 MHz, CD₃OD) δ 149.3, 148.0, 136.2, 134.4, 132.1, 132.0, 131.6, 130.1, 128.0, 127.8, 127.5, 124.4, 118.8, 116.3, 55.9, 52.4, 47.9, 44.7, 43.5, 39.5, 30.1; ESI MS *m/z* 585.7 (M + H)⁺.

4-(4-Chlorophenyl)-1-[(*S*)-3,4-dihydroxybutyl]-3-(3-[4-[4-(4-[(*R*)-4-(dimethylamino)-1-(phenylthio)but-2-yl]amino]-3-nitrophenylsulfonamido)phenyl]piperazin-1-yl)phenyl)-*N*-[3-(4-methylpiperazin-1-yl)propyl]-1*H*-pyrrole-2-carboxamide (7). Compound **7** was prepared in 24% yield from compounds **15** and **26** by a similar procedure as that used to prepare BM-977. ¹H NMR (300 MHz, CD₃OD) δ 8.30 (d, *J* = 2.2 Hz, 1H), 7.59 (dd, *J* = 2.3, 9.2 Hz, 1H), 7.28 (t, *J* = 7.9 Hz, 1H), 7.18–6.98 (m, 15H), 6.91 (d, *J* = 9.4 Hz, 1H), 6.83 (s, 1H), 6.78 (d, *J* = 7.5 Hz, 1H), 4.38–4.28 (m, 2H), 4.09–4.08 (m, 1H), 3.55–3.32 (m, 11H), 3.21–3.15 (m, 14H), 2.84 (s, 3H), 2.83 (s, 6H), 2.70–2.65 (m, 2H), 2.25–1.99 (m, 3H), 1.78–1.64 (m, 3H); ¹³C NMR (75 MHz, CD₃OD) δ 165.4, 151.7, 147.9, 137.2, 136.2, 135.0, 134.5, 132.6, 132.2, 131.6, 130.7, 130.5, 130.2, 129.3, 129.2, 128.0, 127.9, 127.7, 126.7, 126.1, 124.8, 124.3, 124.1, 123.5, 120.0, 118.8, 116.8, 116.2, 115.8, 70.2, 67.2, 55.9, 55.4, 53.1, 52.4, 51.0, 50.7, 50.5, 46.2, 43.7, 43.5, 39.6, 37.7, 36.4, 30.1, 25.9; ESI MS *m/z* 1107.7 (M + H)⁺.

(*R*)-*N*-[4-[4-(4'-Chloro-[1,1'-biphenyl]-2-yl)methyl]piperazin-1-yl]phenyl]-4-[[4-(dimethylamino)-1-(phenylthio)but-2-yl]amino]-3-nitrobenzenesulfonamide (13). Compound **15** (58.5 mg, 0.1 mmol) and 4'-chloro-[1,1'-biphenyl]-2-carbaldehyde (21.7 mg, 0.1 mmol) were mixed in 1,2-dichloroethane (5 mL) and then treated with sodium triacetoxyborohydride (30 mg, 0.14 mmol). The mixture was stirred at room temperature under N₂ atmosphere for 24 h until the reactants were consumed. Then the reaction mixture was quenched by adding 1 N NaOH, and the product was extracted with CH₂Cl₂. The CH₂Cl₂ extract was washed with brine and dried over MgSO₄. The solvent was evaporated and purified by HPLC to give **13** (61 mg, 78%). ¹H NMR (300 MHz, CD₃OD) δ 8.24 (s, 1H), 7.70–7.68 (m, 1H), 7.58–7.47 (m, 5H), 7.39–7.31 (m, 3H), 7.12 (d, *J* = 7.0 Hz, 2H), 7.02–6.89 (m, 6H), 8.18

(d, *J* = 8.7 Hz, 2H), 4.40 (s, 2H), 4.08 (m, 1H), 3.38–3.31 (m, 3H), 3.21–3.08 (m, 9H), 2.84 (s, 6H), 2.25–2.15 (m, 2H); ¹³C NMR (75 MHz, CD₃OD) δ 148.6, 147.9, 144.4, 139.7, 136.2, 135.3, 134.4, 132.6, 132.3, 132.2, 132.1, 131.6, 131.4, 130.2, 130.1, 130.0, 128.0, 127.8, 127.6, 127.5, 124.3, 118.6, 116.2, 58.0, 55.9, 52.8, 52.4, 47.5, 43.5, 39.6, 30.1; ESI MS *m/z* 785.8 (M + H)⁺.

4-Fluoro-3-nitro-*N*-phenylbenzenesulfonamide (29). Compound **29** was prepared in 80% yield by a procedure similar to that used to prepare compound **28**. ¹H NMR (300 MHz, CCl₃D) δ 8.51 (dd, *J* = 2.3, 6.8 Hz, 1H), 8.02–7.97 (m, 1H), 7.42–7.30 (m, 3H), 7.14–7.11 (m, 2H), 6.92 (s, 1H).

(*R*)-4-[[4-(Dimethylamino)-1-(phenylthio)but-2-yl]amino]-3-nitro-*N*-phenylbenzenesulfonamide (14). Compound **14** was prepared from **29** by a similar procedure as that used for compound **15**, in 83% yield. ¹H NMR (300 MHz, CD₃OD) δ 8.38 (d, *J* = 2.2 Hz, 1H), 8.15 (d, *J* = 9.3 Hz, 1H), 7.62 (dd, *J* = 2.1, 9.1 Hz, 1H), 7.28–7.23 (m, 2H), 7.18–6.97 (m, 8H), 6.90 (d, *J* = 9.3 Hz, 1H), 4.11–4.07 (m, 1H), 3.40–3.33 (m, 1H), 3.23–3.09 (m, 3H), 2.85 (s, 6H), 2.31–2.11 (m, 2H); ¹³C NMR (75 MHz, CD₃OD) δ 147.9, 139.0, 136.1, 134.4, 132.3, 131.5, 130.3, 128.0, 127.9, 127.7, 125.8, 121.8, 116.1, 55.9, 52.3, 43.5, 39.4, 30.1; ESI MS *m/z* 501.7 (M + H)⁺.

(*R*)-*N*-[4-[[4-(Dimethylamino)-1-(phenylthio)butan-2-yl]amino]-3-nitrophenyl]sulfonyl]-4-ethynylbenzamide (30). A suspension of **5** (400 mg, 0.94 mmol), 4-ethynylbenzoic acid (138 mg, 0.94 mmol), (dimethylamino)pyridine (DMAP; 230 mg, 1.88 mmol), and EDCI (362 g, 1.88 mmol) in CH₂Cl₂ (10 mL) was stirred at room temperature for 8 h. The reaction mixture was washed with saturated NH₄Cl (3 × 8 mL) and concentrated. The crude residue was purified by HPLC to provide **30** (365 mg, 70%). ¹H NMR (300 MHz, CD₃OD) δ 8.66 (s, 1H), 8.30 (d, *J* = 9.2 Hz, 1H), 7.89 (d, *J* = 8.0 Hz, 2H), 7.52 (d, *J* = 8.0 Hz, 2H), 7.21–7.19 (m, 2H), 7.05–6.89 (m, 4H), 4.16–4.15 (m, 1H), 3.80 (s, 1H), 3.40–3.34 (m, 1H), 3.24–3.13 (m, 3H), 2.86 (s, 6H), 2.30–2.14 (m, 2H); ¹³C NMR (75 MHz, CD₃OD) δ 165.5, 147.2, 134.8, 134.1, 132.0, 131.6, 130.7, 130.1, 128.7, 128.5, 128.0, 127.4, 126.5, 125.4, 114.6, 81.8, 81.0, 54.5, 51.1, 42.2, 38.0, 28.7; ESI MS *m/z* 553.8 (M + H)⁺.

4-(4-Chlorophenyl)-1-[(*S*)-3,4-dihydroxybutyl]-3-[3-[[4-[[4-[(*R*)-4-(dimethylamino)-1-(phenylthio)but-2-yl]amino]-3-nitrophenyl]sulfonyl]carbonyl]phenyl]-ethynyl]phenyl)-*N*-[3-(4-methylpiperazin-1-yl)propyl]-1*H*-pyrrole-2-carboxamide (9). CuI (6.9 mg, 0.036 mmol) and Pd(PPh₃)₄ (13.9 mg, 0.012 mmol) were added to a solution of **26** (83 mg, 0.12 mmol), **30** (66 mg, 0.12 mmol), and Et₃N (50 μL, 0.36 mmol) in DMF (5 mL) at room temperature under nitrogen. The mixture was stirred at 40 °C for 3 h and then filtered through Celite, washed with 50 mL of CH₂Cl₂, and concentrated under reduced pressure. The residue was resolved in MeOH (5 mL) and treated with 0.2 mL of HCl solution (4 M in dioxane) for 10 min, and then the solvent was removed in vacuum. Purification of the residue by HPLC afforded **9** (97 mg, 75%). ¹H NMR (300 MHz, CD₃OD) δ 8.70 (d, *J* = 1.9 Hz, 1H), 7.94 (d, *J* = 7.4 Hz, 1H), 7.83 (d, *J* = 8.3 Hz, 2H), 7.58 (d, *J* = 8.2 Hz, 2H), 7.48 (d, *J* = 7.7 Hz, 1H), 7.38–7.34 (m, 2H), 7.24–7.01 (m, 12H), 4.37–4.29 (m, 2H), 4.19–4.17 (m, 1H), 3.56–3.39 (m, 8H), 3.27–3.13 (m, 9H), 2.87–2.76 (m, 11H), 2.31–2.22 (m, 2H), 2.04–2.01 (m, 1H), 1.75–1.70 (m, 3H); ¹³C NMR (75 MHz, CD₃OD) δ 166.9, 165.4, 148.6, 136.8, 136.2, 135.5, 134.8, 134.7, 132.9, 132.8, 132.6, 132.2, 131.5, 130.6, 130.1, 129.9, 129.5, 129.4, 129.3,

127.9, 126.9, 126.8, 125.0, 124.7, 123.9, 123.5, 93.4, 89.6, 70.2, 67.3, 55.9, 55.5, 52.6, 52.5, 50.4, 46.1, 43.6, 39.4, 37.7, 36.4, 30.1, 25.7; ESI MS m/z 1075.8 (M + H)⁺.

(R)-4-[[4-(Dimethylamino)-1-(phenylthio)but-2-yl]-amino]-N-(4-ethynylphenyl)-3-nitrobenzenesulfonamide (31). Compound 31 was prepared by a similar procedure to that used for compound 30 in 80% yield. ¹H NMR (300 MHz, CD₃OD) δ 8.43 (s, 1H), 7.64 (d, J = 8.8 Hz, 1H), 7.38 (d, J = 8.2 Hz, 2H), 7.21–7.14 (m, 4H), 7.10–6.93 (m, 4H), 4.13–4.12 (m, 1H), 3.44–3.37 (m, 2H), 3.26–3.14 (m, 3H), 2.88 (s, 6H), 2.30–2.21 (m, 2H); ¹³C NMR (75 MHz, CD₃OD) δ 146.7, 138.0, 134.7, 132.9, 132.7, 130.9, 130.1, 128.7, 126.6, 126.5, 125.9, 119.6, 118.3, 114.9, 82.4, 77.3, 54.5, 51.0, 42.1, 38.0, 28.7; ESI MS m/z 526.0 (M + H)⁺.

4-(4-Chlorophenyl)-1-[(S)-3,4-dihydroxybutyl]-3-(3-[[4-(4-[(R)-4-(dimethylamino)-1-(phenylthio)but-2-yl]-amino]-3-nitrophenylsulfonamido)phenyl]ethynyl)phenyl)-N-[3-(4-methylpiperazin-1-yl)propyl]-1H-pyrrole-2-carboxamide (10). Compound 10 was prepared from 31 by a similar procedure as that for 9 in 79% yield. ¹H NMR (300 MHz, CD₃OD) δ 8.39 (d, J = 2.2 Hz, 1H), 7.63 (dd, J = 2.2, 9.0 Hz, 1H), 7.40–7.37 (m, 3H), 7.32–7.27 (m, 2H), 7.15–7.10 (m, 8H), 7.01–6.89 (m, 6H), 4.37–4.21 (m, 2H), 4.09–4.06 (m, 1H), 3.53–3.49 (m, 1H), 3.45–3.43 (m, 2H), 3.33–3.31 (m, 5H), 3.24–3.08 (m, 9H), 2.82 (s, 9H), 2.72–2.68 (m, 2H), 2.24–1.98 (m, 3H), 1.79–1.63 (m, 3H); ¹³C NMR (75 MHz, CD₃OD) δ 165.4, 148.1, 139.4, 136.6, 136.2, 134.8, 134.4, 134.3, 133.7, 132.7, 132.2, 132.0, 131.5, 131.2, 130.5, 130.1, 129.8, 129.3, 128.0, 127.9, 127.4, 126.7, 125.2, 124.7, 124.6, 123.5, 121.1, 120.1, 116.3, 90.2, 90.0, 70.2, 67.3, 55.9, 55.4, 52.7, 52.3, 50.5, 46.1, 43.6, 43.5, 39.4, 37.6, 36.4, 30.1, 25.7; ESI MS m/z 1048.4 (M + H)⁺.

(S)-3-(3-Azidophenyl)-4-(4-chlorophenyl)-1-[2-(2,2-dimethyl-1,3-dioxolan-4-yl)ethyl]-N-[3-(4-methylpiperazin-1-yl)propyl]-1H-pyrrole-2-carboxamide (32). A mixture of 26 (300 mg, 0.43 mmol), sodium azide (42 mg, 0.65 mmol), CuI (8.3 mg, 0.043 mmol), L-proline (10 mg, 0.087 mmol), and NaOH (3.5 mg, 0.087 mmol) in DMSO (4 mL) in a sealed tube was heated to 70 °C under N₂. After the reaction was completed, the cooled mixture was partitioned between CH₂Cl₂ and H₂O. The organic layer was separated, and the aqueous layer was extracted twice with CH₂Cl₂. The combined organic layers were washed with brine, dried over Mg₂SO₄, and concentrated in vacuo. The residue was purified by flash chromatography on silica gel to afford 32 (134 mg, 51%). ¹H NMR (300 MHz, CCl₃D) δ 7.35–7.29 (m, 1H), 7.11 (d, J = 8.3 Hz, 2H), 6.98 (d, J = 7.7 Hz, 2H), 6.93–6.87 (m, 4H), 5.54 (br s, 1H), 4.47–4.43 (m, 1H), 4.38–4.29 (m, 1H), 4.10–4.08 (m, 1H), 4.03–3.00 (m, 1H), 3.53 (t, J = 7.3 Hz, 1H), 3.21–3.15 (m, 2H), 2.36–1.96 (m, 15H), 1.42–1.40 (m, 5H), 1.32 (s, 3H); ¹³C NMR (75 MHz, CCl₃D) δ 161.5, 140.6, 136.8, 132.8, 131.8, 130.2, 129.1, 128.4, 127.2, 124.1, 123.8, 122.2, 121.2, 118.1, 108.9, 73.2, 69.1, 55.7, 54.9, 52.7, 46.3, 45.8, 37.8, 35.7, 27.0, 26.1, 25.6; ESI MS m/z 606.8 (M + H)⁺.

4-(4-Chlorophenyl)-1-[(S)-3,4-dihydroxybutyl]-3-(3-[4-(4-[(R)-4-(dimethylamino)-1-(phenylthio)but-2-yl]-amino]-3-nitrophenylsulfonamido)phenyl]-1H-1,2,3-triazol-1-yl)phenyl)-N-[3-(4-methylpiperazin-1-yl)propyl]-1H-pyrrole-2-carboxamide (8). Compounds 32 (90 mg, 0.15 mmol) and 31 (78 mg, 0.15 mmol) were suspended in a 1:2 mixture of H₂O and *t*-BuOH (9 mL), and then a solution of CuSO₄·5H₂O (3.7 mg, 0.015 mmol) and (+)-sodium L-ascorbate (8.8 mg, 0.045 mmol) in H₂O (1 mL) was added.

The resulting mixture was stirred at room temperature overnight and then was diluted with water (10 mL) and extracted with CH₂Cl₂ (3 × 20 mL). The combined organic layer was washed with brine, dried over Na₂SO₄, and concentrated under reduced pressure. The residue was resolved in MeOH (5 mL) and treated with HCl solution (4 M in dioxane, 0.2 mL) for 10 min, and then the solvent was removed in vacuum. Purification of the residue by HPLC afforded 8 (97 mg, 75%). ¹H NMR (300 MHz, CD₃OD) δ 8.67 (s, 1H), 8.38 (d, J = 2.2 Hz, 1H), 7.78–7.70 (m, 4H), 7.62 (dd, J = 2.2, 9.2 Hz, 1H), 7.47 (t, J = 7.0 Hz, 1H), 7.24–7.21 (m, 3H), 7.12–7.01 (m, 7H), 6.94–6.88 (m, 4H), 4.35–4.28 (m, 2H), 4.07–4.06 (m, 1H), 3.54–3.34 (m, 9H), 3.20–3.11 (m, 8H), 2.84–2.80 (m, 11H), 2.19–2.15 (m, 3H), 1.71–1.66 (m, 3H); ¹³C NMR (75 MHz, CD₃OD) δ 165.4, 148.9, 148.1, 139.3, 138.3, 138.0, 136.1, 134.7, 134.3, 132.9, 132.4, 132.2, 131.5, 131.0, 130.8, 130.0, 129.4, 128.1, 127.8, 127.7, 127.4, 127.1, 124.8, 124.5, 123.6, 123.4, 121.9, 120.1, 119.9, 116.4, 70.2, 67.3, 55.9, 55.5, 52.4, 50.3, 46.1, 43.5, 39.4, 37.7, 36.4, 30.1, 25.7; ESI MS m/z 1091.4 (M + H)⁺.

Ethyl 4-(4-Chlorophenyl)-3-(4-iodophenyl)-1H-pyrrole-2-carboxylate. Compound 33 was prepared by a similar procedure as was used to prepare 24 in 58% yield in two steps. ¹H NMR (300 MHz, CCl₃D) δ 9.52 (br s, 1H), 7.56 (d, J = 8.2 Hz, 2H), 7.20 (d, J = 8.4 Hz, 2H), 7.09 (d, J = 3.0 Hz, 1H), 7.04–7.01 (m, 4H), 4.23 (q, J = 7.1 Hz, 2H), 1.20 (t, J = 7.1 Hz, 3H); ¹³C NMR (75 MHz, CCl₃D) δ 161.0, 136.8, 133.7, 132.7, 132.2, 129.6, 128.5, 127.9, 125.5, 120.4, 120.2, 92.9, 60.5, 14.1.

(S)-Ethyl 4-(4-Chlorophenyl)-1-[2-(2,2-dimethyl-1,3-dioxolan-4-yl)ethyl]-3-(4-iodophenyl)-1H-pyrrole-2-carboxylate (34). Compound 34 was prepared from 33 by a procedure similar to that used for 25 in 90% yield. ¹H NMR (300 MHz, CCl₃D) δ 7.62 (d, J = 8.4 Hz, 2H), 7.16 (d, J = 8.6 Hz, 2H), 7.05 (s, 1H), 6.98–6.93 (m, 4H), 4.62–4.55 (m, 1H), 4.46–4.36 (m, 1H), 4.15–4.03 (m, 4H), 3.63–3.57 (m, 1H), 2.21–2.12 (m, 1H), 2.08–1.94 (m, 1H), 1.47 (s, 3H), 1.38 (s, 3H), 0.99 (t, J = 7.1 Hz, 3H); ¹³C NMR (75 MHz, CCl₃D) δ 161.2, 136.7, 135.4, 132.6, 131.9, 130.0, 129.3, 128.4, 126.4, 123.0, 119.9, 109.1, 92.3, 73.1, 69.0, 60.0, 46.8, 35.5, 27.0, 25.6, 13.7.

(S)-Ethyl 4-(4-Chlorophenyl)-1-[2-(2,2-dimethyl-1,3-dioxolan-4-yl)ethyl]-3-[4-(4-nitrophenyl)piperazin-1-yl]phenyl]-1H-pyrrole-2-carboxylate (35). Compound 34 (380 mg, 0.66 mmol), 1-(4-nitrophenyl)piperazine (271 mg, 1.31 mmol), CuI (12 mg, 0.066 mmol), L-proline (15 mg, 0.13 mmol), and K₂CO₃ (181 mg, 1.31 mmol) were dissolved in 5 mL of DMSO. This mixture was heated to 80 °C for 2 h under nitrogen. After the solution was cooled, saturated ammonium chloride solution was added and the mixture was extracted with CH₂Cl₂. The combined organic layers were washed with brine, dried over sodium sulfate, and concentrated. Purification of the residue by flash chromatography on silica gel afforded 35 (354 mg, 82%). ¹H NMR (300 MHz, CCl₃D) δ 8.15 (d, J = 8.9 Hz, 2H), 7.15–7.11 (m, 4H), 7.05–7.00 (m, 3H), 6.90–6.87 (m, 4H), 4.63–4.54 (m, 1H), 4.45–4.36 (m, 1H), 4.12–4.04 (m, 4H), 3.62–3.57 (m, 5H), 3.39–3.37 (m, 4H), 2.21–2.15 (m, 1H), 2.09–2.00 (m, 1H), 1.47 (s, 3H), 1.38 (s, 3H), 1.02 (t, J = 7.1 Hz, 3H); ¹³C NMR (75 MHz, CCl₃D) δ 161.5, 154.7, 149.4, 138.6, 133.2, 131.5, 131.1, 129.3, 128.3, 127.5, 126.4, 126.0, 123.1, 120.0, 115.3, 112.7, 109.1, 73.2, 69.1, 59.8, 48.9, 47.1, 46.9, 35.6, 27.0, 25.6, 13.8; ESI MS m/z 659.8 (M + H)⁺.

(S)-4-(4-Chlorophenyl)-1-[2-(2,2-dimethyl-1,3-dioxolan-4-yl)ethyl]-N-[3-(4-methylpiperazin-1-yl)propyl]-3-[4-[4-(4-nitrophenyl)piperazin-1-yl]phenyl]-1H-pyrrole-2-carboxamide (36). Compound 36 was prepared from 35 in 85% yield in two steps by a procedure similar to that used for 26. ¹H NMR (300 MHz, CCl₃D) δ 8.14 (d, *J* = 8.9 Hz, 2H), 7.17–7.10 (m, 4H), 6.89–6.86 (m, 7H), 5.61 (t, *J* = 5.3 Hz, 1H), 4.58–4.49 (m, 1H), 4.44–4.35 (m, 1H), 4.13–4.09 (m, 1H), 4.05–4.01 (m, 1H), 3.62–3.53 (m, 5H), 3.41–3.40 (m, 4H), 3.18 (q, *J* = 6.2 Hz, 2H), 2.35–1.98 (m, 15H), 1.48–1.40 (m, 5H), 1.35 (s, 3H); ¹³C NMR (75 MHz, CCl₃D) δ 161.8, 154.5, 149.8, 138.7, 133.4, 131.7, 131.4, 129.1, 128.3, 126.0, 125.8, 125.0, 124.2, 123.5, 122.3, 116.0, 112.8, 108.9, 73.4, 69.1, 55.8, 55.0, 53.0, 48.2, 47.0, 46.5, 45.9, 37.5, 35.7, 27.0, 26.4, 25.7; ESI MS *m/z* 770.4 (M + H)⁺.

4-(4-Chlorophenyl)-1-[(S)-3,4-dihydroxybutyl]-3-[4-[4-(4-[(R)-4-(dimethylamino)-1-(phenylthio)but-2-yl]amino)-3-nitrophenylsulfonamido]phenyl]piperazin-1-yl]phenyl]-N-[3-(4-methylpiperazin-1-yl)propyl]-1H-pyrrole-2-carboxamide (12). Pd–C (10%; 20 mg) was added to a solution of compound 36 (124 mg, 0.16 mmol) in CH₂Cl₂ (3 mL) and MeOH (3 mL). The solution was stirred under 1 atm of H₂ at room temperature for 0.5 h before it was filtered through Celite and concentrated. The resulting aniline was used in the next step without purification. To this aniline in pyridine (5 mL) was added 4-fluoro-3-nitrobenzene-1-sulfonyl chloride (39 mg, 0.16 mmol) at 0 °C. The mixture was stirred at 0 °C for 30 min. The pyridine was removed under vacuum and the residue was purified by flash chromatography on silica gel to give (S)-4-(4-chlorophenyl)-1-[2-(2,2-dimethyl-1,3-dioxolan-4-yl)ethyl]-3-[4-[(2-[(4-(4-fluoro-3-nitrophenylsulfonamido)phenyl]amino)ethyl]amino]phenyl]-N-[3-(4-methylpiperazin-1-yl)propyl]-1H-pyrrole-2-carboxamide. *N,N*-Diisopropylethylamine (DIEA; 56 μL, 0.32 mmol) was added to a solution of this sulfonamide and (*R*)-*N*¹,*N*¹-dimethyl-4-(phenylthio)butane-1,3-diamine (39 mg, 0.16 mmol) in DMF. The solution was stirred overnight and concentrated. The residue was dissolved in MeOH (5 mL) and treated with HCl solution (4 M in dioxane, 0.2 mL) for 10 min, and then the solvent was removed in vacuum. Purification of the residue by HPLC afforded 12 (94 mg, 51% in four steps). ¹H NMR (300 MHz, CD₃OD) δ 8.36 (s, 1H), 7.66 (d, *J* = 9.1 Hz, 1H), 7.22–7.04 (m, 18H), 6.97 (d, *J* = 9.2 Hz, 1H), 4.43–4.31 (m, 2H), 4.15–4.13 (m, 1H), 3.59–3.37 (m, 17H), 3.26–3.21 (m, 8H), 2.90–2.82 (m, 11H), 2.30–2.05 (m, 3H), 1.83–1.74 (m, 3H); ¹³C NMR (75 MHz, CD₃OD) δ 165.6, 147.9, 136.2, 135.1, 134.4, 132.7, 132.5, 132.3, 131.6, 130.5, 130.1, 129.2, 128.0, 127.9, 127.7, 126.3, 125.9, 125.1, 124.2, 123.7, 119.2, 117.9, 116.2, 70.3, 67.3, 55.9, 55.5, 52.5, 52.4, 51.4, 50.6, 50.4, 46.3, 43.6, 43.5, 39.5, 37.5, 36.5, 30.1, 25.7; ESI MS *m/z* 1107.7 (M + H)⁺.

(S)-Ethyl 4-(4-Chlorophenyl)-1-[2-(2,2-dimethyl-1,3-dioxolan-4-yl)ethyl]-3-[3-[(2-[(4-nitrophenyl)amino]ethyl]amino)phenyl]-1H-pyrrole-2-carboxylate (37). Compound 37 was prepared in 78% yield from 26 by a procedure similar to that used for 35. ¹H NMR (300 MHz, CCl₃D) δ 8.07 (d, *J* = 8.6 Hz, 2H), 7.15–7.13 (m, 3H), 7.05–7.02 (m, 3H), 6.66 (d, *J* = 7.5 Hz, 1H), 6.59 (d, *J* = 8.5 Hz, 1H), 6.52 (d, *J* = 8.8 Hz, 2H), 6.46 (s, 1H), 4.58–4.56 (m, 1H), 4.45–4.35 (m, 1H), 4.11–3.99 (m, 4H), 3.59 (t, *J* = 6.9 Hz, 1H), 3.37 (br s, 4H), 2.18–2.16 (m, 1H), 2.06–2.01 (m, 1H), 1.47 (s, 3H), 1.38 (s, 3H), 1.01 (t, *J* = 7.1 Hz, 3H); ¹³C NMR (75 MHz, CCl₃D) δ 161.5, 153.3, 146.9, 138.1, 136.9, 133.1, 131.6, 129.2, 128.6, 128.2, 126.4, 126.2, 122.8, 121.1, 120.0, 115.3, 111.9,

109.1, 73.2, 69.1, 59.8, 46.8, 43.0, 42.5, 35.5, 27.0, 25.6, 13.7; ESI MS *m/z* 633.4 (M + H)⁺.

4-(4-Chlorophenyl)-1-[(S)-3,4-dihydroxybutyl]-3-[3-[(2-[(4-(4-[(R)-4-(dimethylamino)-1-(phenylthio)but-2-yl]amino)-3-nitrophenylsulfonamido]phenyl]amino)ethyl]amino]phenyl]-N-[3-(4-methylpiperazin-1-yl)propyl]-1H-pyrrole-2-carboxamide (11). Compound 11 was prepared from 37 in 40% yield over six steps by a procedure similar to that used for compound 12. ¹H NMR (300 MHz, CD₃OD) δ 8.35 (d, *J* = 1.9 Hz, 1H), 7.65 (d, *J* = 7.4 Hz, 1H), 7.33–6.94 (m, 14H), 6.78–6.61 (m, 5H), 4.45–4.31 (m, 2H), 4.15–4.12 (m, 1H), 3.70–3.39 (m, 8H), 3.28–3.17 (m, 13H), 2.90–2.88 (m, 9H), 2.69–2.64 (m, 2H), 2.30–2.05 (m, 3H), 1.85–1.82 (m, 1H), 1.70–1.68 (m, 2H); ¹³C NMR (75 MHz, CD₃OD) 165.2, 147.9, 137.6, 136.2, 135.0, 134.5, 132.5, 132.3, 131.6, 130.9, 130.3, 130.1, 129.2, 128.02, 127.96, 127.7, 125.9, 125.1, 125.0, 123.4, 116.2, 70.2, 67.3, 55.9, 55.4, 53.0, 52.3, 50.7, 46.4, 43.7, 43.5, 39.6, 37.6, 36.4, 30.1, 25.8; ESI MS *m/z* 1081.6 (M + H)⁺.

Ethyl 4-(4-Chlorophenyl)-3-(3-iodophenyl)-1-methyl-1H-pyrrole-2-carboxylate (38). K₂CO₃ (1.83 g, 13.3 mmol) and MeI (1.89 g, 13.3 mmol) were added to a solution of 24 (3.0 g, 6.6 mmol) in DMF (40 mL). The reaction mixture was stirred for 4 h under nitrogen at room temperature. Then the reaction was diluted with water (40 mL) and extracted with EtOAc (2 × 60 mL). The combined organics were washed with water (60 mL) and brine (60 mL) and then dried over Na₂SO₄. After evaporation of the solvent, the residue was purified by flash chromatography on silica gel to provide 38 (2.88 g, 93%). ¹H NMR (300 MHz, CCl₃D) δ 7.64 (t, *J* = 1.6 Hz, 1H), 7.60 (dt, *J* = 1.6, 7.8 Hz, 1H), 7.15–7.12 (m, 2H), 7.07–7.04 (m, 1H), 7.00–6.91 (m, 4H), 4.06 (q, *J* = 7.1 Hz, 2H), 3.97 (s, 3H), 1.00 (t, *J* = 7.1 Hz, 3H); ¹³C NMR (75 MHz, CCl₃D) δ 161.6, 139.8, 138.2, 135.7, 132.8, 132.0, 129.42, 129.39, 129.0, 128.5, 127.0, 122.9, 121.0, 93.4, 60.1, 37.8, 14.0.

Ethyl 4-(4-Chlorophenyl)-1-methyl-3-[3-[4-(4-nitrophenyl)piperazin-1-yl]phenyl]-1H-pyrrole-2-carboxylate (39). Compound 39 was prepared in 83% yield by a procedure similar to that used for compound 35. ¹H NMR (300 MHz, CCl₃D) δ 8.12 (d, *J* = 9.1 Hz, 2H), 7.26–7.21 (m, 1H), 7.13 (d, *J* = 8.3 Hz, 2H), 7.03 (d, *J* = 8.3 Hz, 2H), 6.96 (s, 1H), 6.90–6.79 (m, 5H), 4.09 (q, *J* = 7.1 Hz, 2H), 3.99 (s, 3H), 3.54–3.51 (m, 4H), 3.27–3.24 (m, 4H), 1.01 (t, *J* = 7.1 Hz, 3H); ¹³C NMR (75 MHz, CCl₃D) δ 161.7, 154.7, 150.1, 138.5, 136.7, 133.2, 131.5, 131.0, 129.2, 128.4, 128.2, 126.6, 125.9, 123.1, 122.7, 121.0, 119.0, 114.9, 112.7, 59.8, 49.0, 46.9, 37.6, 13.8; ESI MS *m/z* 545.8 (M + H)⁺.

(R)-4-(4-Chlorophenyl)-3-[3-[4-[4-(4-[(dimethylamino)-1-(phenylthio)but-2-yl]amino)-3-nitrophenylsulfonamido]phenyl]piperazin-1-yl]phenyl]-1-methyl-1H-pyrrole-2-carboxylic acid (20). Compound 20 was prepared from 38 in 49% yield in four steps by a procedure similar to that used for 12. ¹H NMR (300 MHz, CD₃OD) δ 8.29 (d, *J* = 2.2 Hz, 1H), 7.58 (dd, *J* = 2.3, 9.2 Hz, 1H), 7.27 (t, *J* = 7.8 Hz, 1H), 7.15–6.89 (m, 18H), 4.08–4.05 (m, 1H), 3.93 (s, 3H), 3.67–3.30 (m, 9H), 3.20–3.14 (m, 3H), 2.82 (s, 6H), 2.23–2.14 (m, 2H); ¹³C NMR (75 MHz, CD₃OD) δ 164.3, 147.9, 138.9, 136.2, 134.8, 134.4, 132.8, 132.6, 132.2, 131.7, 131.6, 130.6, 130.1, 130.0, 129.2, 128.7, 128.3, 128.0, 127.9, 127.6, 124.1, 124.0, 122.4, 122.0, 119.1, 117.8, 116.2, 55.9, 52.8, 52.4, 50.6, 43.5, 39.5, 38.1, 30.1; ESI MS *m/z* 895.1 (M + H)⁺.

(R)-4-(4-Chlorophenyl)-3-[3-[4-[4-(4-[(dimethylamino)-1-(phenylthio)but-2-yl]amino)-3-nitrophenylsulfonamido]phenyl]piperazin-1-yl]phenyl]-1-methyl-N-[3-(4-methylpiperazin-1-yl)propyl]-1H-pyrrole-2-carboxamide (16). A mixture of 20 (76 mg, 0.085 mmol), 1-(3-aminopropyl)-4-methylpiperazine (20 mg, 0.127 mmol), EDCI (24.5 mg,

0.127 mmol), HOBt (16.4 mg, 0.127 mol), and DIEA (44 μ L, 0.25 mmol) in DCM (5 mL) was stirred for 8 h and then concentrated. The residue was purified by HPLC to provide **16** (74 mg, 84%). ^1H NMR (300 MHz, CD_3OD) δ 8.30 (d, $J = 2.2$ Hz, 1H), 7.59 (dd, $J = 2.2, 9.1$ Hz, 1H), 7.28 (t, $J = 7.9$ Hz, 1H), 7.16–6.89 (m, 16H), 6.82–6.77 (m, 2H), 4.09–4.06 (m, 1H), 3.82 (s, 3H), 3.33–3.28 (m, 6H), 3.25–3.09 (m, 16H), 2.83 (s, 9H), 2.62–2.57 (m, 2H), 2.24–2.14 (m, 2H), 1.65–1.61 (m, 2H); ^{13}C NMR (75 MHz, CD_3OD) δ 165.1, 151.6, 147.9, 137.4, 136.2, 135.0, 134.4, 132.5, 132.2, 131.6, 130.7, 130.4, 130.1, 129.2, 128.0, 127.9, 127.6, 126.7, 126.4, 125.8, 124.2, 123.3, 120.1, 118.9, 116.9, 116.2, 55.9, 55.4, 52.9, 52.4, 51.1, 50.6, 50.5, 43.6, 43.5, 39.5, 37.5, 36.3, 30.1, 25.9; ESI MS m/z 1033.7 ($\text{M} + \text{H}$) $^+$.

(R)-4-(4-Chlorophenyl)-3-(3-[4-[4-(4-(dimethylamino)-1-(phenylthio)but-2-yl]amino)-3-nitrophenylsulfonamido]phenyl]piperazin-1-yl]phenyl)-N,1-dimethyl-1H-pyrrole-2-carboxamide (17). A mixture of **20** (42 mg, 0.047 mmol), 2 M methylamine in THF (47 μ M, 0.094 mmol), EDCI (18.0 mg, 0.094 mmol), HOBt (12.1 mg, 0.094 mol), and DIEA (25 μ L, 0.14 mmol) in DCM (3 mL) was stirred for 8 h and then concentrated. The residue was purified by HPLC to provide **17** (36.6 mg, 86%). ^1H NMR (300 MHz, CD_3OD) δ 8.32 (d, $J = 1.2$ Hz, 1H), 7.58 (d, $J = 9.1$ Hz, 1H), 7.28 (t, $J = 7.9$ Hz, 1H), 7.17–6.99 (m, 15H), 6.90 (d, $J = 9.3$ Hz, 1H), 6.86 (s, 1H), 6.80 (d, $J = 7.5$ Hz, 1H), 4.09–4.07 (m, 1H), 3.80 (s, 3H), 3.45–3.33 (m, 9H), 3.21–3.08 (m, 3H), 2.84 (s, 6H), 3.05 (s, 3H), 2.25–2.10 (m, 2H); ^{13}C NMR (75 MHz, CD_3OD) δ 165.4, 149.9, 148.0, 147.2, 137.4, 136.2, 135.1, 134.4, 133.6, 132.6, 132.3, 131.6, 130.7, 130.6, 130.1, 129.2, 128.0, 127.9, 127.6, 126.9, 125.9, 125.8, 125.6, 124.0, 123.1, 120.8, 119.5, 117.4, 116.2, 55.9, 52.4, 51.4, 43.5, 39.6, 36.2, 30.1, 26.4; ESI MS m/z 907.6 ($\text{M} + \text{H}$) $^+$.

(R)-N-[4-(4-[3-[4-(4-Chlorophenyl)-1-methyl-1H-pyrrol-3-yl]phenyl]piperazin-1-yl]phenyl)-4-[[4-(dimethylamino)-1-(phenylthio)but-2-yl]amino]-3-nitrobenzenesulfonamide (18). TFA (0.5 mL) was added to a solution of **20** (37 mg, 0.041 mmol) in DCM (2 mL). The solution was stirred for 15 min and then evaporated. The residue was purified by HPLC to afford compound **18** (28 mg, 80%). ^1H NMR (300 MHz, CD_3OD) δ 8.30 (d, $J = 2.2$ Hz, 1H), 7.59 (dd, $J = 2.2, 9.2$ Hz, 1H), 7.25 (m, 1H), 7.18–6.89 (m, 17H), 6.80 (dd, $J = 2.3, 9.7$ Hz, 2H), 4.10–4.06 (m, 1H), 3.67 (s, 3H), 3.35–3.30 (m, 9H), 3.20–3.14 (m, 3H), 2.82 (s, 6H), 2.23–2.14 (m, 2H); ^{13}C NMR (75 MHz, CD_3OD) δ 148.0, 147.9, 139.3, 136.3, 136.2, 134.4, 133.0, 132.34, 132.25, 131.6, 131.0, 130.8, 130.1, 129.3, 128.0, 127.9, 127.6, 126.0, 124.1, 123.6, 123.4, 123.2, 123.1, 123.0, 119.7, 119.2, 116.8, 116.2, 55.9, 53.0, 52.4, 50.5, 43.5, 39.5, 36.4, 30.1; ESI MS m/z 851.6 ($\text{M} + \text{H}$) $^+$.

(R)-Ethyl 4-(4-Chlorophenyl)-3-(3-[4-[4-(4-(dimethylamino)-1-(phenylthio)but-2-yl]-amino)-3-nitrophenylsulfonamido]phenyl]piperazin-1-yl]phenyl)-1-methyl-1H-pyrrole-2-carboxylate (19). A mixture of **20** (37 mg, 0.041 mmol), EtOH (1 mL), N,N' -diisopropylcarbodiimide (16 mg, 0.124 equiv), and 4-(dimethylamino)pyridine (1.0 mg, 0.008 mmol) in THF (3 mL) was stirred for 8 h and then concentrated. The residue was purified by HPLC to provide **19** (29 mg, 76%). ^1H NMR (300 MHz, CD_3OD) δ 8.31 (d, $J = 2.1$ Hz, 1H), 7.60 (dd, $J = 2.1, 9.1$ Hz, 1H), 7.31 (t, $J = 7.8$ Hz, 1H), 7.17–6.90 (m, 18H), 4.11–4.07 (m, 1H), 3.99 (q, $J = 7.1$ Hz, 2H), 3.93 (s, 3H), 3.39–3.31 (m, 9H), 3.21–3.14 (m, 3H), 2.83 (s, 6H), 2.27–2.11 (m, 2H), 0.93 (t, $J = 7.1$ Hz, 3H); ^{13}C NMR (75 MHz, CD_3OD) δ 162.9, 148.0, 139.1, 136.2, 134.6,

134.4, 133.3, 132.7, 132.3, 131.6, 130.5, 130.1, 130.0, 129.2, 128.6, 128.0, 127.9, 127.6, 124.0, 123.9, 122.0, 121.9, 119.4, 117.7, 116.2, 60.9, 55.9, 52.44, 52.37, 51.0, 43.5, 39.5, 37.8, 30.1, 14.2; ESI MS m/z 922.8 ($\text{M} + \text{H}$) $^+$.

Ethyl 5-Bromo-4-(4-chlorophenyl)-3-(3-iodophenyl)-1-methyl-1H-pyrrole-2-carboxylate (40). *N*-Bromosuccinimide (0.59 g, 3.3 mmol) was added in portions to a solution of **24** (1.5 g, 3.3 mmol) in DMF (20 mL) and the resulting mixture was stirred at room temperature for 2 h. The reaction mixture was diluted with H_2O (30 mL) and extracted into EtOAc (2×30 mL). The combined organics were washed with water (30 mL) and brine (30 mL) and dried over Na_2SO_4 . After removal of the solvent under vacuum, a solution of the residue in DMF (20 mL) was added to K_2CO_3 (0.92 g, 6.6 mmol) and MeI (0.94 g, 6.6 mmol). This reaction mixture was stirred for 4 h under nitrogen at room temperature. The reaction was diluted with water (20 mL) and extracted into EtOAc (2×30 mL). The combined organics were washed with water (30 mL) and then brine (30 mL) and dried over Na_2SO_4 . After evaporation of the solvent, the residue was purified by flash chromatography on silica gel to provide **40** (1.3 g, 71% yield over two steps). ^1H NMR (300 MHz, CCl_3D) δ 7.61 (s, 1H), 7.56 (d, $J = 7.5$ Hz, 1H), 7.21 (d, $J = 8.4$ Hz, 2H), 7.05 (d, $J = 8.4$ Hz, 2H), 6.99–6.89 (m, 2H), 4.09 (q, $J = 7.1$ Hz, 2H), 4.05 (s, 3H), 1.01 (t, $J = 7.1$ Hz, 3H); ^{13}C NMR (75 MHz, CCl_3D) δ 160.9, 139.7, 137.2, 135.7, 132.8, 131.7, 131.5, 130.0, 129.7, 129.1, 128.2, 123.6, 121.7, 111.7, 93.1, 60.3, 35.6, 13.8.

Ethyl 5-Bromo-4-(4-chlorophenyl)-1-methyl-3-[3-[4-(4-nitrophenyl)piperazin-1-yl]phenyl]-1H-pyrrole-2-carboxylate (41). Compound **41** was prepared in 74% yield by a procedure similar to that used for compound **35**. ^1H NMR (300 MHz, CCl_3D) δ 8.15 (d, $J = 9.3$ Hz, 2H), 7.21–7.14 (m, 3H), 7.07 (d, $J = 8.5$ Hz, 2H), 6.87–6.81 (m, 3H), 6.72 (d, $J = 7.6$ Hz, 1H), 6.63 (s, 1H), 4.09 (q, $J = 7.1$ Hz, 2H), 4.04 (s, 3H), 3.53–3.49 (m, 4H), 3.20–3.17 (m, 4H), 0.99 (t, $J = 7.1$ Hz, 3H); ^{13}C NMR (75 MHz, CCl_3D) δ 161.20, 154.7, 149.8, 138.6, 135.6, 132.5, 132.1, 131.9, 131.7, 128.2, 128.1, 125.9, 123.6, 123.1, 121.7, 119.1, 114.9, 112.7, 111.3, 60.1, 48.9, 46.9, 35.5, 13.8; ESI MS m/z 623.3 ($\text{M} + \text{H}$) $^+$.

Ethyl 4-(4-Chlorophenyl)-1-methyl-3-[3-[4-(4-nitrophenyl)piperazin-1-yl]phenyl]-5-[(trimethylsilyl)ethynyl]-1H-pyrrole-2-carboxylate (42). CuI (37 mg, 0.19 mmol) and $\text{Pd}(\text{PPh}_3)_4$ (111 mg, 0.096 mmol) were added to a solution of **41** (600 mg, 0.96 mmol), ethynyltrimethylsilane (473 mg, 4.8 mmol), and Et_3N (0.4 mL, 2.9 mmol) in DMF (20 mL) in a sealed tube at room temperature under nitrogen. After being stirred at 80 $^\circ\text{C}$ for 6 h, the reaction mixture was cooled and filtered through Celite, washed with 50 mL of CH_2Cl_2 , and concentrated under reduced pressure. Purification of the residue by flash chromatography on silica gel afforded **42** (160 mg, 26%). ^1H NMR (300 MHz, CCl_3D) δ 8.15 (d, $J = 9.3$ Hz, 2H), 7.23–7.14 (m, 5H), 6.87–6.84 (m, 3H), 6.74 (d, $J = 7.6$ Hz, 1H), 6.69 (s, 1H), 4.09 (q, $J = 7.1$ Hz, 2H), 4.06 (s, 3H), 3.54–3.51 (m, 4H), 3.24–3.21 (m, 4H), 0.99 (t, $J = 7.1$ Hz, 3H), 0.26 (s, 9H); ^{13}C NMR (75 MHz, CCl_3D) δ 161.2, 154.7, 150.0, 138.7, 135.9, 132.1, 130.9, 130.4, 128.4, 127.8, 127.5, 125.9, 123.2, 121.7, 119.7, 119.1, 114.9, 112.7, 103.9, 95.3, 60.1, 49.0, 46.9, 34.9, 13.7, -0.26 ; ESI MS m/z 641.9 ($\text{M} + \text{H}$) $^+$.

4-(4-Chlorophenyl)-5-ethynyl-1-methyl-3-[3-[4-(4-nitrophenyl)piperazin-1-yl]phenyl]-1H-pyrrole-2-carboxylic acid (43). KOH (56 mg, 1.0 mmol) was added to a solution of **42** (160 mg, 0.25 mmol) in a mixture of dioxane/ $\text{EtOH}/\text{H}_2\text{O}$ (1:1:1, 10 mL) and the solution was refluxed for

2 h. After being cooled, the reaction was neutralized with 1 M HCl and extracted with EtOAc. The EtOAc solution was washed with brine, dried over Na_2SO_4 , and concentrated in vacuum. Purification of the residue by flash chromatography on silica gel afforded **43** (116 mg, 86%). ^1H NMR (300 MHz, CCl_3D) δ 8.15 (d, $J = 9.1$ Hz, 2H), 7.22–7.10 (m, 5H), 6.86–6.83 (m, 3H), 6.76–6.73 (m, 2H), 4.06 (s, 3H), 3.51–3.49 (m, 5H), 3.22–3.19 (m, 4H); ^{13}C NMR (75 MHz, CCl_3D) δ 154.7, 149.9, 138.7, 134.9, 132.5, 132.1, 131.6, 131.0, 128.6, 128.1, 126.0, 123.1, 120.1, 119.4, 115.2, 112.7, 86.1, 74.2, 48.8, 46.8, 35.5; ESI MS m/z 541.8 ($\text{M} + \text{H}$) $^+$.

(R)-4-(4-Chlorophenyl)-3-(3-[4-[4-(4-(dimethylamino)-1-(phenylthio)but-2-yl]amino)-3-nitrophenylsulfonamido]phenyl]piperazin-1-yl]phenyl)-5-ethyl-1-methyl-1H-pyrrole-2-carboxylic acid (21). Pd–C (10%; 15 mg) was added to a solution of compound **43** (82 mg, 0.15 mmol) in a mixture of CH_2Cl_2 (3 mL) and MeOH (3 mL). The mixture was stirred under 1 atm of H_2 at room temperature for 0.5 h before being filtered through Celite and concentrated. The resulting aniline was used in the next step without purification. To this aniline in pyridine (5 mL) was added 4-fluoro-3-nitrobenzene-1-sulfonyl chloride (36 mg, 0.15 mmol) at 0 °C. The mixture was stirred at 0 °C for 30 min. The pyridine was removed under vacuum and the residue was purified by flash chromatography on silica gel to give 4-(4-chlorophenyl)-5-ethyl-3-(3-[4-[4-(4-fluoro-3-nitrophenylsulfonamido)phenyl]-piperazin-1-yl]phenyl)-1-methyl-1H-pyrrole-2-carboxylic acid. DIEA (53 μL , 0.30 mmol) was added to a solution of this sulfonamide and (R)- N^1,N^1 -dimethyl-4-(phenylthio)butane-1,3-diamine (34 mg, 0.15 mmol) in DMF. The reaction mixture was stirred overnight and concentrated. The residue was resolved in a mixture of H_2O and CH_3CN (a trace of HCl was added to assist with solubility), and purification by HPLC with H_2O and CH_3CN (without TFA) as eluents afforded **21** (41 mg, 29% in four steps). ^1H NMR (300 MHz, CD_3OD) δ 8.34 (d, $J = 1.9$ Hz, 1H), 7.60 (dd, $J = 1.9, 9.1$ Hz, 1H), 7.20–6.93 (m, 16H), 6.83–6.81 (m, 2H), 4.13–4.11 (m, 1H), 3.92 (s, 3H), 3.41–3.35 (m, 2H), 3.24–3.21 (m, 10H), 2.86 (s, 6H), 2.66 (q, $J = 7.5$ Hz, 2H), 2.35–2.13 (m, 2H), 1.16 (t, $J = 7.5$ Hz, 3H); ^{13}C NMR (75 MHz, CD_3OD) δ 164.8, 147.9, 140.3, 138.3, 136.2, 135.6, 134.5, 133.3, 133.1, 132.3, 131.6, 130.1, 129.2, 129.0, 128.0, 127.9, 127.7, 124.5, 123.0, 122.1, 120.3, 118.5, 116.8, 116.2, 56.0, 52.4, 52.1, 50.3, 43.5, 39.6, 33.6, 30.1, 18.9, 14.5; ESI MS m/z 922.5 ($\text{M} + \text{H}$) $^+$.

Fluorescence Polarization-Based Binding Assays. Details of the expression and purification of Bcl-2, Bcl-xL, and Mcl-1 proteins and determination of K_d values of fluorescent probes to proteins are provided in the Supporting Information. IC_{50} and K_i values to Bcl-2/Bcl-xL/Mcl-1 of our synthesized compounds and reference compounds were determined in competitive binding experiments, in which an inhibitor in serial dilutions was allowed to compete with a fixed concentration of a fluorescent probe for a fixed concentration of a protein. Mixtures of 5 μL of the tested compound in DMSO and 120 μL of preincubated protein/probe complex in the assay buffer were added to assay plates and incubated at room temperature for 2 h with gentle shaking. The final concentrations of the protein and probe, respectively, were 1.5 nM and 1 nM for the Bcl-2 assay, 10 nM and 2 nM for the Bcl-xL assay, and 20 nM and 2 nM for the Mcl-1 assay. Controls containing protein/probe complex only (equivalent to 0% inhibition) or free probe only (equivalent to 100% inhibition), were included in each assay plate. FP values were measured as described above. IC_{50} values

were determined by nonlinear regression fitting of the competition curves. The K_i value of a compound to a protein was calculated by use of the equation described previously,²⁶ based upon the measured IC_{50} value, the K_d value of the probe to the protein, and the concentration of the protein and probe in the competitive assays. K_i values were also calculated from an equation published in the literature.²⁷ The values obtained from both equations were found to be in excellent agreement.

Molecular Modeling. Crystal structures of Bcl-xL with **1**¹⁸ (PDB entry 2YXJ) and **4** were used to model the binding poses of our designed compounds with Bcl-xL. In the binding models, the structure of Bcl-xL in complex with **4** was superimposed on that of Bcl-xL in complex with **1**. The core scaffold of **4** then replaced the 4'-chloro-2-methyl-1,1'-biphenyl group of **1** to generate the initial binding model, which was then refined by a 1 ns molecular dynamics (MD) simulation. All the modifications of the ligands were performed by the Sybyl program.²⁸

The charge and force field parameters of the compounds were obtained with the most recent Antechamber module in the Amber 10 program suite,²⁹ where the charge models were calculated from the Gaussian 98 program³⁰ at the Hartree–Fock level by use of the 6-31G** basis sets. Protocols for the MD simulation are the following. The total charge of the system was neutralized by first adding counterions. Then, the system was solvated in a 10 Å cubic box of water by use of the TIP3P water model.³¹ Two thousand steps of minimization of the system were performed where the protein and the modeled compound were constrained by a force constant of 50 $\text{kcal}\cdot\text{mol}^{-1}\cdot\text{Å}^{-2}$. After minimization, a 20 ps simulation was used to gradually raise the temperature of the system to 298 K while the whole system was constrained by a force constant of 10 $\text{kcal}\cdot\text{mol}^{-1}\cdot\text{Å}^{-2}$. Another 40 ps of equilibrium run was used where only the backbone atoms of the protein and the ligand atoms were constrained by a force constant of 2 $\text{kcal}\cdot\text{mol}^{-1}\cdot\text{Å}^{-2}$. A final production run of 1 ns was performed with no constraints on any atoms of the complex structure. When constraints were applied, the initial complex structure was used as a reference structure. All the MD simulations were at NTP. The SHAKE algorithm³² was used to fix the bonds involving hydrogen. The PME method³³ was used and the nonbonded cutoff distance was set at 10 Å. The time step was 2 fs, and the neighboring pairs list was updated in every 20 steps. Final conformations of Bcl-xL in complex with **6** and **7** are shown in Figure S1 in Supporting Information.

Cell Growth Assay. The effect of compounds on cell growth was evaluated by a WST-8 [2-(2-methoxy-4-nitrophenyl)-3-(4-nitrophenyl)-5-(2,4-disulfophenyl)-2H-tetrazolium, monosodium salt] assay (Dojindo Molecular Technologies, Gaithersburg, Maryland). Human small-cell lung cancer cell lines H146 and H1417 were purchased from the American Type Culture Collection (ATCC) and were maintained in RPMI-1640 medium containing 10% fetal bovine serum (FBS). Cells were seeded in 96-well flat bottom cell culture plates at a density of 1×10^4 cells/well with various concentrations of compounds and incubated for 4 days. At the end of incubation, WST-8 dye (20 μL) was added to each well and incubated for an additional 1–2 h, and then the absorbance was measured in a microplate reader (Molecular Devices) at 450 nm. The concentration of compounds that inhibited cell growth by 50% (IC_{50}) was calculated by comparing absorbance in the untreated cells and the cells treated with the compounds by use of the GraphPad Prism software (GraphPad Software, La Jolla, CA). At least three

independent experiments were performed to obtain the standard deviation for each compound in each cell line.

Cell Death Assay. Cell death assays were performed via trypan blue staining. Cells were treated with the indicated compounds. At the end of treatment, cells were collected and stained with trypan blue. Cells that stained blue or morphologically unhealthy cells were scored as dead cells. At least 100 cells were counted for each sample.

Western Blotting. Cells were lysed in radioimmunoprecipitation assay lysis buffer [phosphate-buffered saline containing 1% NP40, 0.5% sodium deoxycholate, and 0.1% sodium dodecyl sulfate (SDS)] supplemented with 1 $\mu\text{mol/L}$ phenylmethanesulfonyl fluoride and 1 protease inhibitor cocktail tablet per 10 mL on ice for 20 min, and lysates were then cleared by centrifugation before protein concentration determination by use of the Bio-Rad protein assay kit according to the manufacturer's instructions. Proteins were electrophoresed onto SDS-containing 4–20% polyacrylamide gels (Invitrogen) and transferred onto poly(vinylidene difluoride) membranes. Following blocking in 5% milk, membranes were incubated with a specific primary antibody, washed, and incubated with horseradish peroxidase-linked secondary antibody (Amersham). The signals were visualized with the chemiluminescent horseradish peroxidase antibody detection reagent (Denville Scientific). Rabbit antibodies against PARP and caspase-3 were from Cell Signaling Technology, and rabbit anti-glyceraldehyde 3-phosphate dehydrogenase (GAPDH) was from Santa Cruz Biotechnology.

Bcl-xL Crystallographic Studies. Expression and purification of Bcl-xL ΔTM ΔLP is described in the Supporting Information. Prior to crystallization, Bcl-xL was incubated with a 5-fold molar excess of compound **4** in the presence of 4% DMSO for 1 h at 4 °C and then concentrated to 7 mg/mL. Crystals of Bcl-xL/**4** were grown by vapor diffusion in a sitting drop tray with 1.2 M sodium citrate and 25 mM 2-(cyclohexylamino)ethanesulfonic acid (CHES) buffer, pH 9.0, as the mother liquor. Crystals did not appear until after the well was opened, perturbed with a loop, and resealed. In the experiment, the crystallization drops contained equal volumes of protein and well solution. Prior to data collection, crystals were cryoprotected in well solution with increasing amounts of glycerol, to a final concentration of 20%, and then flash-frozen in liquid nitrogen.

X-ray data was collected at LS-CAT ID-21-F and G lines at the Advanced Photon Source at Argonne National Lab. Data were processed with HKL2000.³⁴ The Bcl-xL/**4** complex crystallized in the $P4_22_1$ space group and diffracted to 1.7 Å resolution. The structure contained one molecule in the asymmetric unit. The structure of the complex was solved by molecular replacement with Phaser³⁵ by use of a structure of Bcl-xL previously solved in our laboratory as a starting model. Iterative rounds of refinement and model building were completed by use of Buster³⁶ and Coot,³⁷ respectively. The initial $F_o - F_c$ electron density map revealed the presence of the compounds in the binding site of Bcl-xL. Only the three-ring core of **4** was visible in the $F_o - F_c$ electron density map contoured at 3σ . The PRODRG server³⁸ was used to create the starting coordinates and restraint files for the compounds. The current $R_{\text{free}}/R_{\text{work}}$ for the Bcl-xL/**4** structure is 0.2036/0.1854. All amino acids fall into the allowed regions of the Ramachandran plot with 98% in the preferred regions. Data collection and refinement statistics are given in Table S1 in Supporting Information.

■ ASSOCIATED CONTENT

📄 Supporting Information

Additional text, one figure, and one table with experimental procedures and spectral data. This material is available free of charge via the Internet at <http://pubs.acs.org>.

Accession Codes

[†]Coordinates for Bcl-xL complexed with **4** were deposited into the Protein Data Bank under Accession Number 3SPF.

■ AUTHOR INFORMATION

Corresponding Author

*Telephone 734-615-0362; fax 734-647-9647; e-mail shaomeng@umich.edu.

Author Contributions

[§]These authors contributed equally.

Notes

The authors declare the following competing financial interest(s): Ascentage has licensed this class of Bcl-2/Bcl-xL inhibitors from the University of Michigan. Dr. Shaomeng Wang is a co-founder for Ascentage and owns stocks in Ascentage. Dr. Shaomeng Wang also serves as a consultant for Ascentage.

■ ACKNOWLEDGMENTS

This research was supported in part by a grant from the National Cancer Institute, National Institutes of Health (U19CA113317). Use of the Advanced Photon Source was supported by the U.S. Department of Energy, Office of Science, Office of Basic Energy Sciences, under Contract DE-AC02-06CH11357. Use of the LS-CAT Sector 21 was supported by the Michigan Economic Development Corporation and the Michigan Technology Tri-Corridor for the support of this research program (Grant 085P1000817).

■ REFERENCES

- (1) Hanahan, D.; Weinberg, R. A. Hallmarks of cancer: the next generation. *Cell* **2011**, *144* (5), 646–674.
- (2) Ziegler, D. S.; Kung, A. L. Therapeutic targeting of apoptosis pathways in cancer. *Curr. Opin. Oncol.* **2008**, *20* (1), 97–103.
- (3) Reed, J. C. Apoptosis-based therapies. *Nat. Rev. Drug Discovery* **2002**, *1* (2), 111–121.
- (4) Cory, S.; Adams, J. M. The Bcl2 family: regulators of the cellular life-or-death switch. *Nat. Rev. Cancer* **2002**, *2* (9), 647–656.
- (5) Cory, S.; Adams, J. M. Killing cancer cells by flipping the Bcl-2/Bax switch. *Cancer Cell* **2005**, *8* (1), 5–6.
- (6) Labi, V.; Erlacher, M.; Kiessling, S.; Villunger, A. BH3-only proteins in cell death initiation, malignant disease and anticancer therapy. *Cell Death Differ.* **2006**, *13* (8), 1325–1238.
- (7) Lessene, G.; Czabotar, P. E.; Colman, P. M. BCL-2 family antagonists for cancer therapy. *Nat. Rev. Drug Discovery* **2008**, *7* (12), 989–1000.
- (8) Di Micco, S.; Vitale, R.; Pelliccia, M.; Rega, M. F.; Riva, R.; Basso, A.; Bifulco, G. Identification of lead compounds as antagonists of protein Bcl-xL with a diversity-oriented multidisciplinary approach. *J. Med. Chem.* **2009**, *52* (23), 7856–7867.
- (9) Feng, Y.; Ding, X.; Chen, T.; Chen, L.; Liu, F.; Jia, X.; Luo, X.; Shen, X.; Chen, K.; Jiang, H.; Wang, H.; Liu, H.; Liu, D. Design, synthesis, and interaction study of quinazoline-2(1H)-thione derivatives as novel potential Bcl-xL inhibitors. *J. Med. Chem.* **2010**, *53* (9), 3465–3479.
- (10) Wei, J.; Stebbins, J. L.; Kitada, S.; Dash, R.; Placzek, W.; Rega, M. F.; Wu, B.; Cellitti, J.; Zhai, D.; Yang, L.; Dahl, R.; Fisher, P. B.; Reed, J. C.; Pelliccia, M. BI-97C1, an optically pure Apogossypol derivative as pan-active inhibitor of antiapoptotic B-cell lymphoma/

- leukemia-2 (Bcl-2) family proteins. *J. Med. Chem.* **2010**, *53* (10), 4166–4176.
- (11) Wei, J.; Kitada, S.; Stebbins, J. L.; Placzek, W.; Zhai, D.; Wu, B.; Rega, M. F.; Zhang, Z.; Cellitti, J.; Yang, L.; Dahl, R.; Reed, J. C.; Pellecchia, M. Synthesis and biological evaluation of Apogossypolone derivatives as pan-active inhibitors of antiapoptotic B-cell lymphoma/leukemia-2 (Bcl-2) family proteins. *J. Med. Chem.* **2010**, *53* (22), 8000–8011.
- (12) Rega, M. F.; Wu, B.; Wei, J.; Zhang, Z.; Cellitti, J. F.; Pellecchia, M. SAR by interligand nuclear overhauser effects (ILOEs) based discovery of acylsulfonamide compounds active against Bcl-x(L) and Mcl-1. *J. Med. Chem.* **2011**, *54* (17), 6000–6013.
- (13) Oltersdorf, T.; Elmore, S. W.; Shoemaker, A. R.; Armstrong, R. C.; Augeri, D. J.; Belli, B. A.; Bruncko, M.; Deckwerth, T. L.; Dinges, J.; Hajduk, P. J.; Joseph, M. K.; Kitada, S.; Korsmeyer, S. J.; Kunzer, A. R.; Letai, A.; Li, C.; Mitten, M. J.; Nettlesheim, D. G.; Ng, S.; Nimmer, P. M.; O'Connor, J. M.; Oleksijew, A.; Petros, A. M.; Reed, J. C.; Shen, W.; Tahir, S. K.; Thompson, C. B.; Tomaselli, K. J.; Wang, B.; Wendt, M. D.; Zhang, H.; Fesik, S. W.; Rosenberg, S. H. An inhibitor of Bcl-2 family proteins induces regression of solid tumours. *Nature* **2005**, *435* (7042), 677–681.
- (14) Park, C. M.; Bruncko, M.; Adickes, J.; Bauch, J.; Ding, H.; Kunzer, A.; Marsh, K. C.; Nimmer, P.; Shoemaker, A. R.; Song, X.; Tahir, S. K.; Tse, C.; Wang, X.; Wendt, M. D.; Yang, X.; Zhang, H.; Fesik, S. W.; Rosenberg, S. H.; Elmore, S. W. Discovery of an orally bioavailable small molecule inhibitor of prosurvival B-cell lymphoma 2 proteins. *J. Med. Chem.* **2008**, *51* (21), 6902–6915.
- (15) Tse, C.; Shoemaker, A. R.; Adickes, J.; Anderson, M. G.; Chen, J.; Jin, S.; Johnson, E. F.; Marsh, K. C.; Mitten, M. J.; Nimmer, P.; Roberts, L.; Tahir, S. K.; Xiao, Y.; Yang, X.; Zhang, H.; Fesik, S.; Rosenberg, S. H.; Elmore, S. W. ABT-263: a potent and orally bioavailable Bcl-2 family inhibitor. *Cancer Res.* **2008**, *68* (9), 3421–3428.
- (16) Sleeb, B. E.; Czabotar, P. E.; Fairbrother, W. J.; Fairlie, W. D.; Flygare, J. A.; Huang, D. C.; Kersten, W. J.; Koehler, M. F.; Lessene, G.; Lowes, K.; Parisot, J. P.; Smith, B. J.; Smith, M. L.; Souers, A. J.; Street, I. P.; Yang, H.; Baell, J. B. Quinazoline sulfonamides as dual binders of the proteins B-cell lymphoma 2 and B-cell lymphoma extra long with potent proapoptotic cell-based activity. *J. Med. Chem.* **2011**, *54* (6), 1914–1926.
- (17) Muchmore, S. W.; Sattler, M.; Liang, H.; Meadows, R. P.; Harlan, J. E.; Yoon, H. S.; Nettlesheim, D.; Chang, B. S.; Thompson, C. B.; Wong, S. L.; Ng, S. L.; Fesik, S. W. X-ray and NMR structure of human Bcl-xL, an inhibitor of programmed cell death. *Nature* **1996**, *381* (6580), 335–341.
- (18) Lee, E. F.; Czabotar, P. E.; Smith, B. J.; Deshayes, K.; Zobel, K.; Colman, P. M.; Fairlie, W. D. Crystal structure of ABT-737 complexed with Bcl-xL: implications for selectivity of antagonists of the Bcl-2 family. *Cell Death Differ.* **2007**, *14* (9), 1711–1713.
- (19) Bruncko, M.; Oost, T. K.; Belli, B. A.; Ding, H.; Joseph, M. K.; Kunzer, A.; Martineau, D.; McClellan, W. J.; Mitten, M.; Ng, S. C.; Nimmer, P. M.; Oltersdorf, T.; Park, C. M.; Petros, A. M.; Shoemaker, A. R.; Song, X.; Wang, X.; Wendt, M. D.; Zhang, H.; Fesik, S. W.; Rosenberg, S. H.; Elmore, S. W. Studies leading to potent, dual inhibitors of Bcl-2 and Bcl-xL. *J. Med. Chem.* **2007**, *50* (4), 641–662.
- (20) Bullington, J. L.; Wolff, R. R.; Jackson, P. F. Regioselective preparation of 2-substituted 3,4-diaryl pyrroles: a concise total synthesis of ningalin B. *J. Org. Chem.* **2002**, *67* (26), 9439–9442.
- (21) Hartwig, J. F.; Kawatsura, M.; Hauck, S. I.; Shaughnessy, K. H.; Alcazar-Roman, L. M. Room-temperature palladium-catalyzed amination of aryl bromides and chlorides and extended scope of aromatic C–N bond formation with a commercial ligand. *J. Org. Chem.* **1999**, *64* (15), 5575–5580.
- (22) Chinchilla, R.; Najera, C. The Sonogashira reaction: a booming methodology in synthetic organic chemistry. *Chem Rev* **2007**, *107* (3), 874–922.
- (23) Zhu, W.; Ma, D. Synthesis of aryl azides and vinyl azides via proline-promoted CuI-catalyzed coupling reactions. *Chem. Commun.* **2004**, *7*, 888–889.
- (24) Rostovtsev, V. V.; Green, L. G.; Fokin, V. V.; Sharpless, K. B. A stepwise Huisgen cycloaddition process: Copper(I)-catalyzed regioselective “ligation” of azides and terminal alkynes. *Angew. Chem., Int. Ed.* **2002**, *41* (14), 2596–2599.
- (25) Zhang, H.; Cai, Q.; Ma, D. Amino acid promoted CuI-catalyzed C–N bond formation between aryl halides and amines or N-containing heterocycles. *J. Org. Chem.* **2005**, *70* (13), 5164–5173.
- (26) Nikolovska-Coleska, Z.; Wang, R.; Fang, X.; Pan, H.; Tomita, Y.; Li, P.; Roller, P. P.; Krajewski, K.; Saito, N. G.; Stuckey, J. A.; Wang, S. Development and optimization of a binding assay for the XIAP BIR3 domain using fluorescence polarization. *Anal. Biochem.* **2004**, *332* (2), 261–273.
- (27) Huang, X. Fluorescence polarization competition assay: the range of resolvable inhibitor potency is limited by the affinity of the fluorescent ligand. *J. Biomol. Screen.* **2003**, *8* (1), 34–38.
- (28) Sybyl, a molecular modeling system, is supplied by Tripos, Inc., St. Louis, MO 63144.
- (29) Case, D. A.; Darden, T. A.; T., E. Cheatham, I.; Simmerling, C. L.; Wang, J.; Duke, R. E.; Luo, R.; Crowley, M.; Walker, R. C.; Zhang, W.; Merz, K. M.; B.Wang, Hayik, S.; Roitberg, A.; Seabra, G.; Kolossvary, I.; K. F. Wong; Paesani, F.; Vanicek, J.; X.Wu; Brozell, S. R.; Steinbrecher, T.; Gohlke, H.; Yang, L.; Tan, C.; Mongan, J.; Hornak, V.; Cui, G.; Mathews, D. H.; Seetin, M. G.; Sagui, C.; Babin, V.; Kollman, P. A. AMBER10; University of California, San Francisco, 2008.
- (30) Frisch, M. J.; Trucks, G. W.; Schlegel, H. B.; Scuseria, G. E.; Robb, M. A.; Cheeseman, J. R.; Zakrzewski, V. G.; Montgomery, J. A., Jr.; Stratmann, R. E.; Burant, J. C.; Dapprich, S.; Millam, J. M.; Daniels, A. D.; Kudin, K. N.; Strain, M. C.; Farkas, O.; Tomasi, J.; Barone, V.; Cossi, M.; Cammi, R.; Mennucci, B.; Pomelli, C.; Adamo, C.; Clifford, S.; Ochterski, J.; Petersson, G. A.; Ayala, P. Y.; Cui, Q.; Morokuma, K.; Malick, D. K.; Rabuck, A. D.; Raghavachari, K.; Foresman, J. B.; Cioslowski, J.; Ortiz, J. V.; Baboul, A. G.; Stefanov, B. B.; Liu, G.; Liashenko, A.; Piskorz, P.; Komaromi, I.; Gomperts, R.; Martin, R. L.; Fox, D. J.; Keith, T.; Al-Laham, M. A.; Peng, C. Y.; Nanayakkara, A.; Challacombe, M.; Gill, P. M.; Johnson, B.; Chen, W.; Wong, M. M.; Andres, J. L.; Gonzalez, C.; Head-Gordon, M.; Replogle, E. S.; Pople, J. A. Gaussian 98, Revision A-11; Gaussian, Inc.: Pittsburgh, PA, 2001.
- (31) Jorgensen, W. L.; Chandrasekhar, J.; Madura, J. D.; Impey, R. W.; Klein, M. L. Comparison of simple potential functions for simulating liquid water. *J. Chem. Phys.* **1983**, *79* (2), 926–935.
- (32) Ryckaert, J.-P.; Ciccotti, G.; Berendsen, H. J. C. Numerical integration of the Cartesian equations of motion of a system with constraints: Molecular dynamics of n-alkanes. *J. Comput. Phys.* **1977**, *23* (3), 327–341.
- (33) Darden, T.; York, D.; Pedersen, L. Particle mesh Ewald - an N.log(N) method for Ewald sums in large systems. *J. Chem. Phys.* **1993**, *98* (12), 10089–10092.
- (34) Otwinowski, Z.; Minor, W. Processing of X-ray diffraction data collected in oscillation mode. In *Methods in Enzymology*; Carter, C. W., Jr., Ed.; Academic Press: New York, 1997; Vol. 276, pp 307–326.
- (35) McCoy, A. J.; Grosse-Kunstleve, R. W.; Adams, P. D.; Winn, M. D.; Storoni, L. C.; Read, R. J. Phaser crystallographic software. *J. Appl. Crystallogr.* **2007**, *40* (Pt 4), 658–674.
- (36) Bricogne, G.; Blanc, E.; Brandl, M.; Flensburg, C.; Keller, P.; Paciorek, W.; Roversi, P.; Sharff, A.; Smart, O.; Vonrhein, C.; Womack, T. BUSTER, version 2.9; Global Phasing Ltd., Cambridge, U.K., 2010.
- (37) Emsley, P.; Cowtan, K. Coot: model-building tools for molecular graphics. *Acta Crystallogr. D: Biol. Crystallogr.* **2004**, *60*, 2126–2132.
- (38) Schuttelkopf, A. W.; van Aalten, D. M. PRODRG: a tool for high-throughput crystallography of protein-ligand complexes. *Acta Crystallogr. D: Biol. Crystallogr.* **2004**, *60* (Pt 8), 1355–1363.